Fermilab Neutrino University Series:

Neutrino (and electron) cross sections and neutrino oscillation experiments

Camillo Mariani
Center for Neutrino Physics, Virginia Tech

Motivation and Contents

- Little bit of theory and connenction with experiments - CCQE cross section and form factors
- Why do we care about cross section and nuclear models ? Determination of neutrino oscillation parameters requires knowledge of neutrino energy
- Modern experiments use complicated nuclear targets: from Carbon to Argon
- A simple way to build and validate a nuclear model for DUNE: the Jefferson Lab E12-14-012 experiment

Bottom line: there is no such thing as an *ab initio* method to describe the properties of atomic nuclei

- In the low-energy regime, the fundamental theory of strong interactions (QCD) becomes nearly intractable already at the level required for the description of isolated hadrons, let alone nuclei

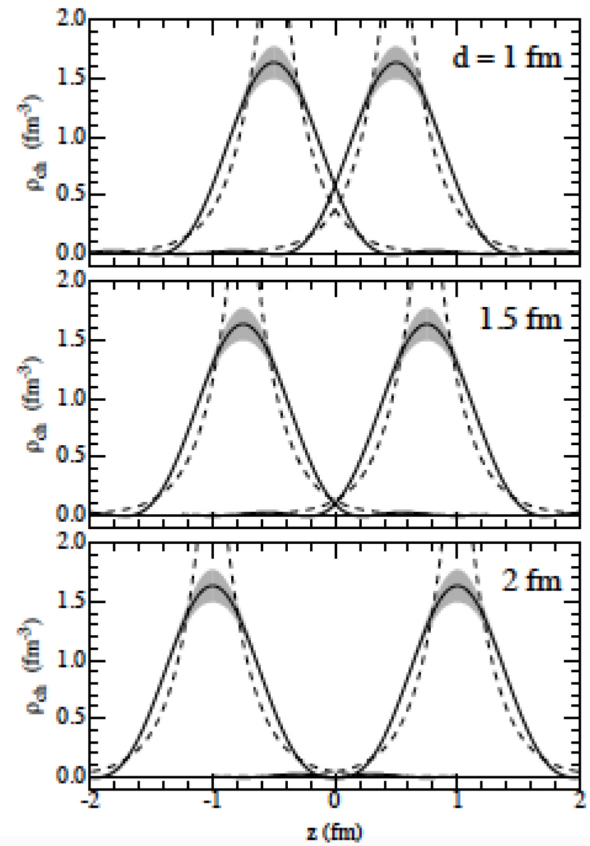

* Nuclei are described in terms of *effective degrees of freedom*, protons and neutrons, and *effective interactions*, mainly meson exchange processes
* As long as their size is small compared to the relative distance, treating nucleons as individual particles appears to be reasonable

Paradigm of Nuclear Many-Body Theory

- ★ Nuclear matter is described as a collection of pointlike protons and neutrons interacting through the hamiltonian

$$H = \sum_i \frac{p_i^2}{2m} + \sum_{j>i} \mathrm{v}_{ij} + \sum_{k>j>i} \mathrm{V}_{\mathrm{ijk}}$$

- ★ The mean field approximation, underlying the nuclear shell model, amounts to replacing

$$\sum_{j>i} \mathrm{v}_{ij} + \sum_{k>j>i} \mathrm{V}_{\mathrm{ijk}} \to \sum_i U_i \ ,$$

- ★ While being able to explain a number of nuclear properties, the mean field approximation fails to take into account correlations, which have long being recognized to play a significant role.

Many-Body Theory of Nuclear Matter

- ⋆ Owing to the presence of a strong repulsive core, the matrix elements of the nuclear Hamiltonian between eigenstates of the Hamiltonian describing the non-interacting system are large. Perturbation theory *in this basis* is not applicable.
- ⋆ Alternate avenues
  - ▸ Replace the bare NN potential with a well behaved *effective interaction*, that can be used in perturbation theory using the Fermi gas basis
    - ▸ G-matrix perturbation theory

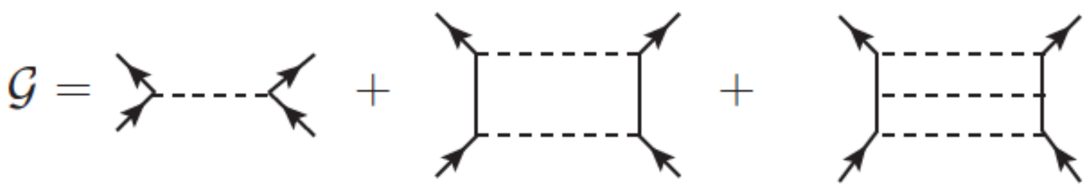

    - ▸ Renormalization group evolution of the bare interaction to low momentum
  - ▸ Modify the basis states in such a way as to mitigate the effects of the repulsive core

Results of Nuclear Many-Body Theory

- ⋆ Quantum Monte Carlo and variational calculations performed using phenomenological nuclear Hamiltonians explain the energies of the ground- and low-lying excited states of nuclei with mass $A \leq 12$, as well as saturation of the equation of state of cold isospin-symmetric nuclear matter

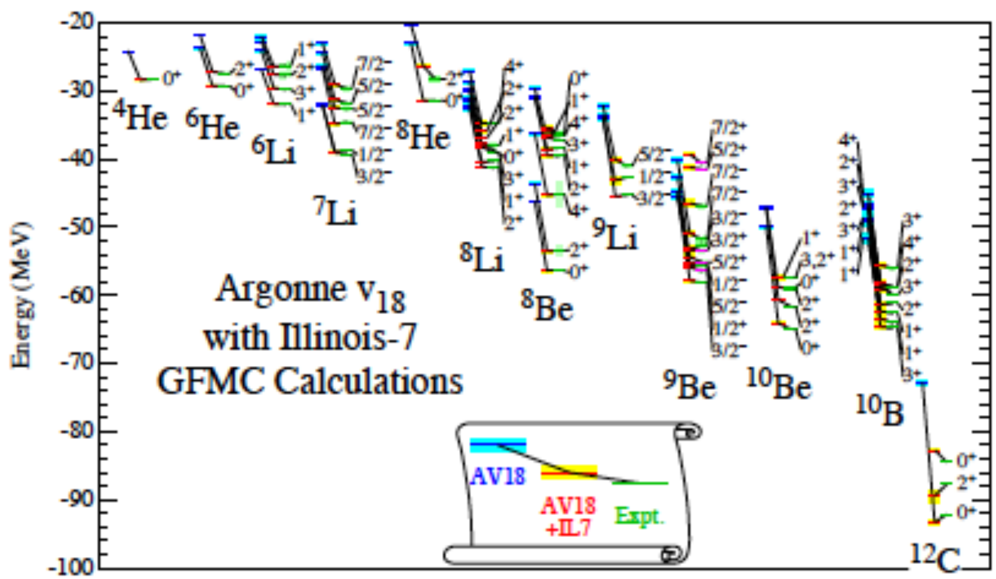

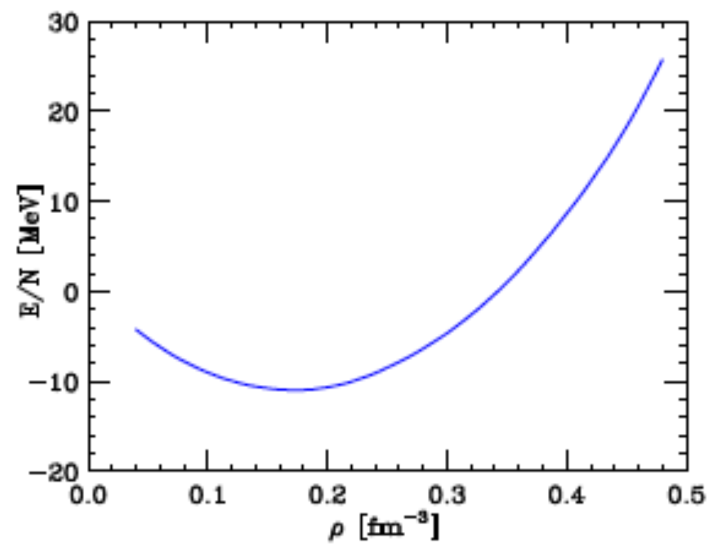

Neutrino-Nucleus Cross-Section

- In the regime of momentum transfer (q) discussed in this Lectures, Fermi theory of weak interaction works just fine

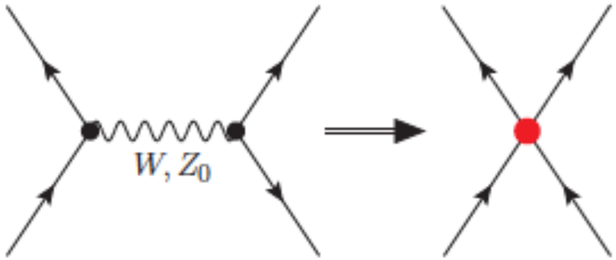

- Consider, for example, the x-section of the charged-current process $\nu_\ell + n \to \ell^- + X$

$$d\sigma \propto L_{\lambda\mu} W^{\lambda\mu}$$

  - $L_{\lambda\mu}$ is determined by the lepton kinematical variables (more on this later)
  - under very general assumptions $W^{\lambda\mu}$ can be written in the form

$$W^{\lambda\mu} = -g^{\lambda\mu} W_1 + p^\lambda p^\mu \frac{W_2}{m_N^2} + i\,\varepsilon^{\lambda\mu\alpha\beta} q_\alpha p_\beta + \frac{W_3}{m_N^2} + q^\lambda q^\mu \frac{W_4}{m_N^2} + (p^\lambda q^\mu + p^\mu q^\lambda) \frac{W_5}{m_N^2}$$

- In principle, the structure functions W_i can be extracted from the measured cross sections
- In the elastic sector $\nu_\ell + n \to \ell^- + p$ they can be expressed in terms of vector ($F_1(q^2)$ and $F_2(q^2)$), axial ($F_A(q^2)$) and pseudoscalar ($F_P(q^2)$) *form factors*

$$W_1 = 2\left[-\frac{q^2}{2}\,(F_1+F_2)^2 + \left(2\,m_N^2 - \frac{q^2}{2}\right)\,{F_A}^2\right]$$

$$W_2 = 4\left[{F_1}^2 - \left(\frac{q^2}{4\,m_N^2}\right)\,{F_2}^2 + {F_A}^2\right] = 2W_5$$

$$W_3 = -4\,(F_1+F_2)\,F_A$$

$$W_4 = -2\left[F_1\,F_2 + \left(2\,m_N^2 + \frac{q^2}{2}\right)\frac{{F_2}^2}{4\,m_N^2} + \frac{q^2}{2}\,{F_P}^2 - 2\,m_N\,F_P\,F_A\right]$$

- according to the CVC hypothesis, F_1 and F_2 can be related to the electromagnetic form factors, measured by electron-nucleon scattering, while PCAC allows one to express F_P in terms of the axial form factor

Vector Form Factor

- ★ Proton data

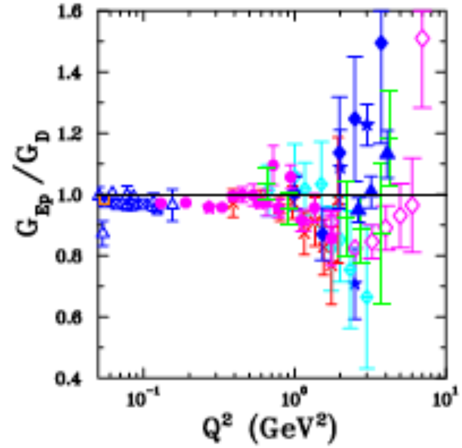

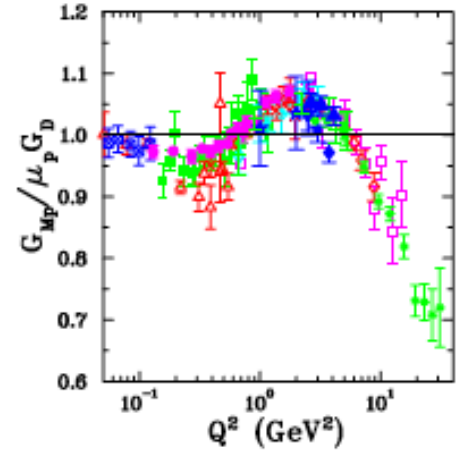

- ★ Neutron (deuteron) data

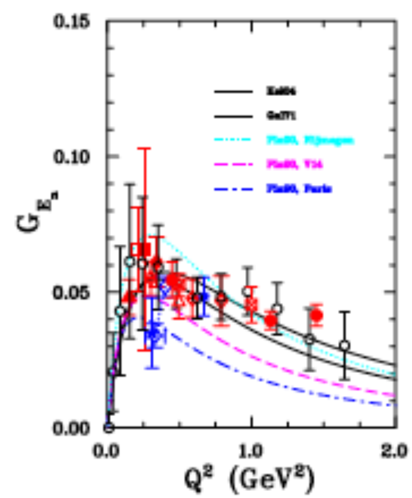

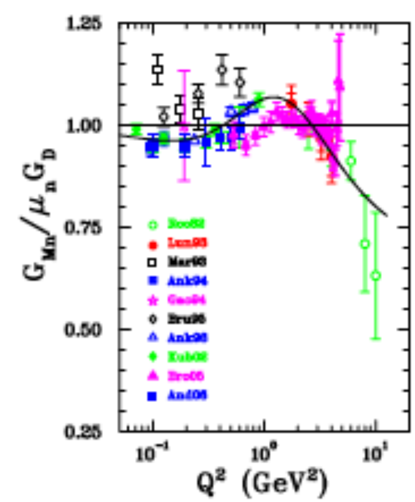

Axial Form Factor

★ Dipole parametrization

$$F_A(Q^2) = \frac{g_A}{[1 + (Q^2/M_A^2)]^2}$$

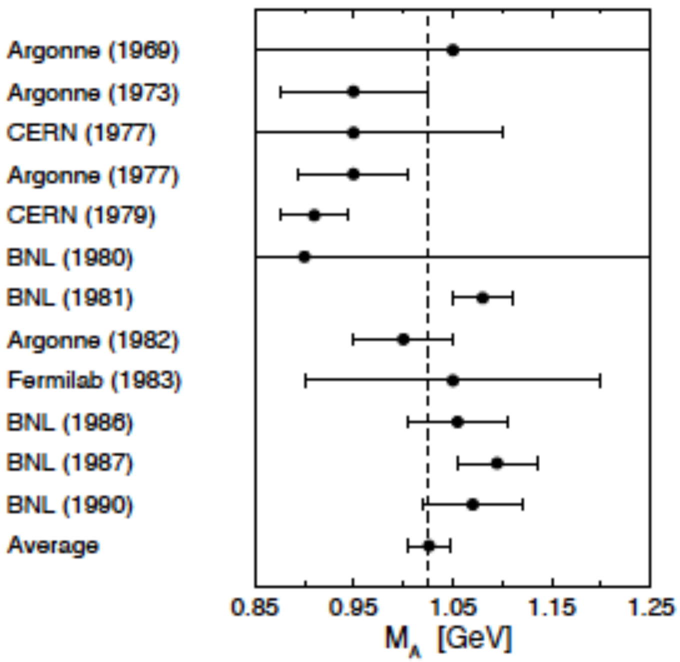

▷ g_A from neutron β-decay

▷ axial mass M_A from (quasi) elastic ν- and $\bar{\nu}$-deuteron experiment

Neutrino-Nucleus Cross-Section

- Consider again a charged current process

$$\nu_\ell + A \to \ell^- + X$$

- Nuclear response tensor

$$W_{\lambda\mu} = \sum_N \langle 0|J_\lambda^\dagger|n\rangle\langle n|J_\mu|0\rangle \delta^{(4)}(p + k - p_N - k')$$

- To take into account all relevant reaction processes one needs to:
  - Model nuclear dynamics
  - Solve the many-body Schrödinger equation $H|n\rangle = E_n|n\rangle$
  - Determine the nuclear weak current (Are the nucleon weak structure functions modified by the nuclear medium? Are there additional contributions to the current?)

Neutrino-Nucleus Cross-Section

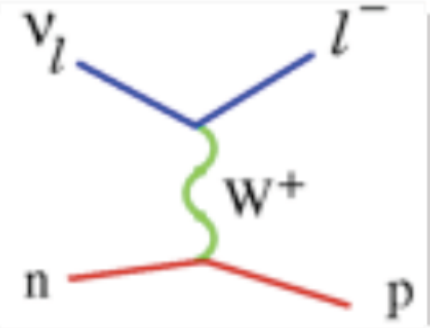

- ⋆ Double differential cross section of the process

$$\nu_\ell(k) + A \to \ell^-(k') + X$$

$$\frac{d^2\sigma}{d\Omega_\ell dE_\ell} = \frac{G_F^2\, V_{ud}^2}{16\,\pi^2}\,\frac{|\mathbf{k}'|}{|\mathbf{k}|}\, L_{\mu\nu}\, W_A^{\mu\nu}\ ,$$

$$L_{\mu\nu} = 8\left[k'_\mu\, k_\nu + k'_\nu\, k_\mu - g_{\mu\nu}(k\cdot k') - i\,\varepsilon_{\mu\nu\alpha\beta}\, k'^{\beta}\, k^{\alpha}\right]$$

- ▸ The determination of the nuclear response tensor

$$W_A^{\mu\nu} = \sum_N \langle 0|J_A^{\mu\,\dagger}|N\rangle\langle N|J_A^{\nu}|0\rangle\delta^{(4)}(P_0 + k - P_N - k')$$

requires a *consistent* description of the target initial and final states and the nuclear current operator

$$J_A^\mu = \sum_i j_i^\mu + \sum_{j>i} j_{ij}^\mu$$

Quasi-Elastic (CCQE) Neutrino-Nucleus Cross-Section

- We use the free nucleon CCQE formalism

$$\frac{d\sigma}{dQ^2_{QE}} = \frac{M^2 G_F^2 \cos^2\theta_C}{8\pi E_\nu^2}\{A(Q^2) \pm B(Q^2)\frac{s-u}{M^2} + C(Q^2)\frac{(s-u)^2}{M^4}\}$$

- Sign on B term is minus for neutrinos, plus for antineutrinos
- G_F is the Fermi constant, 1.17×10^{-5} GeV^2
- M is the average nucleon mass, 938.92 MeV
- θ_C is the Cabbibo angle $cos\theta_C = 0.9742$
- E is the neutrino energy
- s and u s are Mandelstam variables

CCQE-Neutrino-Nucleus Cross-Section

- We use the free nucleon CCQE formalism

$$\frac{d\sigma}{dQ^2_{QE}} = \frac{M^2 G_F^2 \cos^2\theta_C}{8\pi E_\nu^2}\{A(Q^2) \pm B(Q^2)\frac{s-u}{M^2} + C(Q^2)\frac{(s-u)^2}{M^4}\}$$

- Where

$$\begin{aligned} A(Q^2) = \frac{m_\mu^2 - Q^2}{M^2} \Big\{ & (1+\frac{Q^2}{4M^2})F_A^2 - (1-\frac{Q^2}{4M^2})F_1^2 - \frac{Q^2}{4M^2}(1-\frac{Q^2}{4M^2})(\xi F_2)^2 \\ & + \frac{Q^2}{M^2} Re(F_1^* \xi F_2) - \frac{Q^2}{M^2}(1+\frac{Q^2}{4M^2})(F_A^3)^2 \\ & - \frac{m_\mu^2}{4M^2}\left[|F_1 + \xi F_2|^2 + |F_A + 2F_P|^2 - 4(1+\frac{Q^2}{4M^2})((F_V^3)^2 + F_P^2)\right] \Big\} \end{aligned}$$

$$B(Q^2) = \frac{Q^2}{M^2} Re\,[F_A^*(F_1 + \xi F_2)] - \frac{m_\mu^2}{M^2} Re\left[(F_1 - \tau\xi F_2)F_V^{3*} - (F_A^* - \frac{Q^2}{2M^2}F_P)F_A^3)\right]$$

$$C(Q^2) = \frac{1}{4}\left\{F_A^2 + F_1^2 + \tau(\xi F_2)^2 + \frac{Q^2}{M^2}(F_A^3)^2\right\}$$

- Most of the form factors are known, except the axial form factor F_A. This is parameterized as a dipole

$$F_A(Q^2) = \frac{F_A(0)}{(1 - \frac{q^2}{M_A^2})^2}$$

Electron Scattering

- Vast supply of precise data available

$$Q^2 = 4E_eE_{e'}\sin^2\frac{\theta_e}{2} \quad , \quad x = \frac{Q^2}{2M\omega}$$

- Carbon target

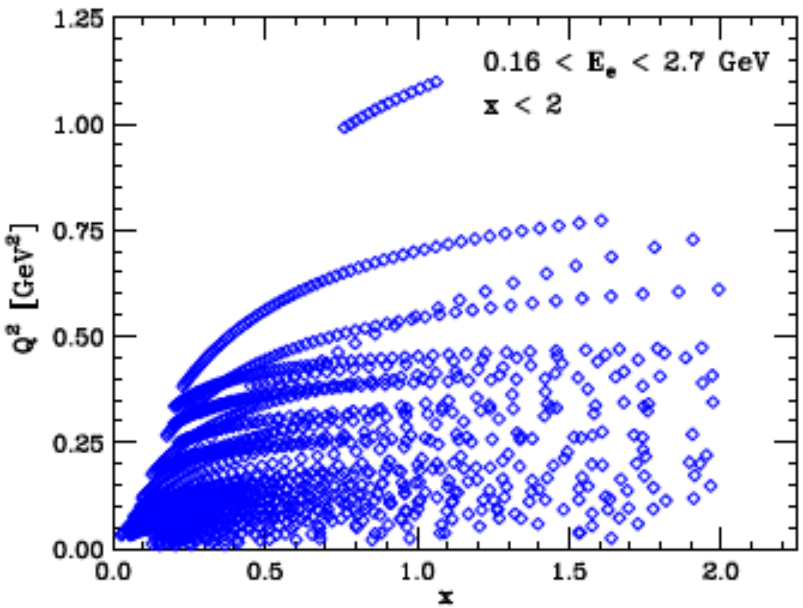

- Different rection mechanisms contributimg to the mesured cross sections can be readily identified

$$e + A \rightarrow e' + X$$

$$E_e \sim 1\ \mathrm{GeV}$$

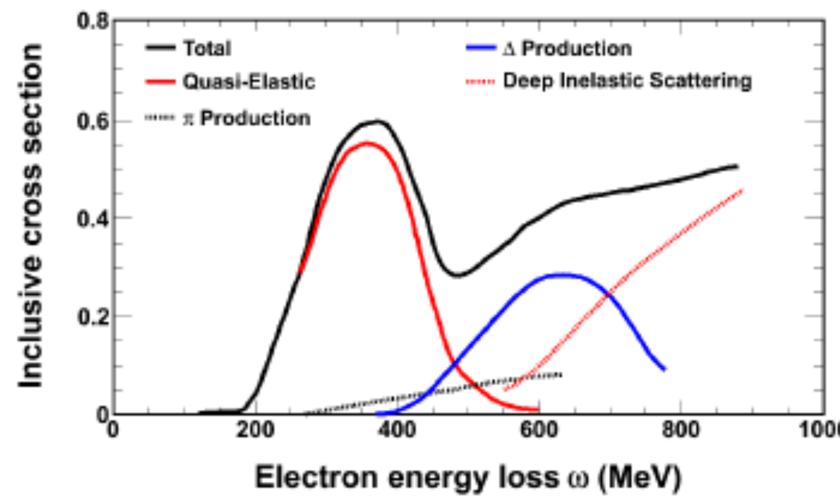

Mean Field

- Nuclear systematics offers ample evidence supporting the further assumption, underlying the nuclear shell model, that the potentials appearing in the Hamiltonian can be eliminated in favour of a mean field

$$H \to H_{MF} = \sum_i \left[\frac{\mathbf{p}_i^2}{2m} + U_i \right]$$

$$\left[\frac{\mathbf{p}_i^2}{2m} + U_i \right] \phi_{\alpha_i} = \epsilon_{\alpha_i} \phi_{\alpha_i} \quad , \quad \alpha \equiv \{n, \ell, j\}$$

- For proposing and developing the nuclear shell model, E. Wigner, M. Goeppert Mayer and J.H.D. Jensen have been awarded the 1963 Nobel Prize in Physics
- A warning from Blatt & Weiskopf (AD 1952): "The limitation of any independent particle model lies in its inability to encompass the correlation between the positions and spins of the various particles in the system"

Shell Model Ground State

- According to the shell model, in the nuclear groud state protons and neutrons occupy the A lowest energy eigenstates of the mean field Hamiltonian

$$H_{MF}\Psi_0 = E_0\Psi_0 \quad , \quad \Psi_0 = \frac{1}{A!}\det\{\phi_\alpha\} \quad , \quad E_0 = \sum_{\alpha\in\{F\}} \epsilon_\alpha$$

- Ground state of ^{16}O: $Z = N = 8$

$$(1S_{1/2})^2 \;\; , \;\; (1P_{3/2})^4 \;\; , \;\; (1P_{1/2})^2$$

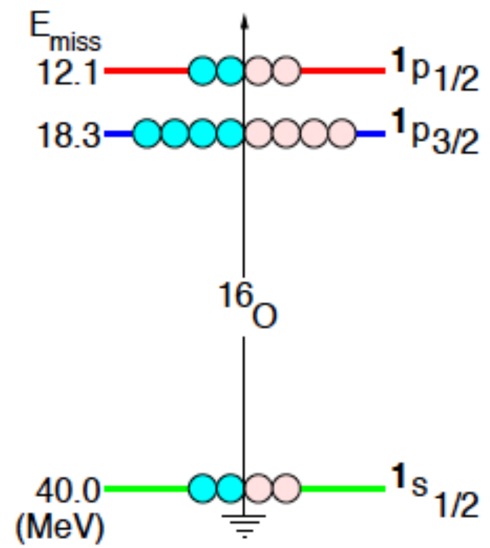

(e, e'p) Reaction

- Consider the process $e + A \to e' + p + (A-1)$ in which both the outgoing electron and the proton, carrying momentum p', are detected in coincidence

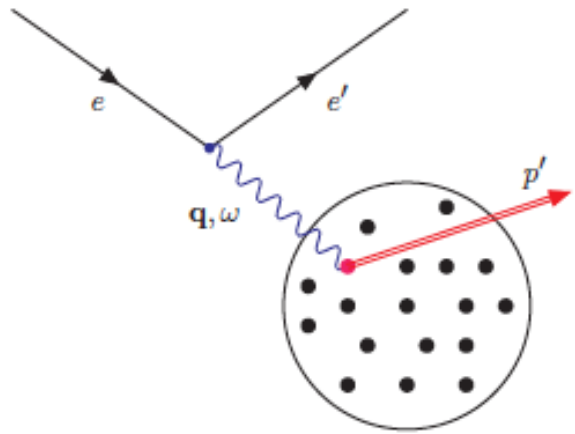

- Assuming that there are no final state interactions (FSI), the initial energy and momentum of the knocked out nucleon can be identified with the *measured* missing momentum and energy, respectively

$$\mathbf{p}_m = \mathbf{p}' - \mathbf{q} \quad , \quad E_m = \omega - T_{\mathbf{p}'} - T_{A-1} \approx \omega - T_{\mathbf{p}'}$$

(e, e'p) Reaction – Proton Knockout from Shell-Model

- The spectral lines corresponding to the shell model states clearly seen in the missing energy spectra of measured by

$$e + \mathrm{A} \rightarrow e' + p + X$$

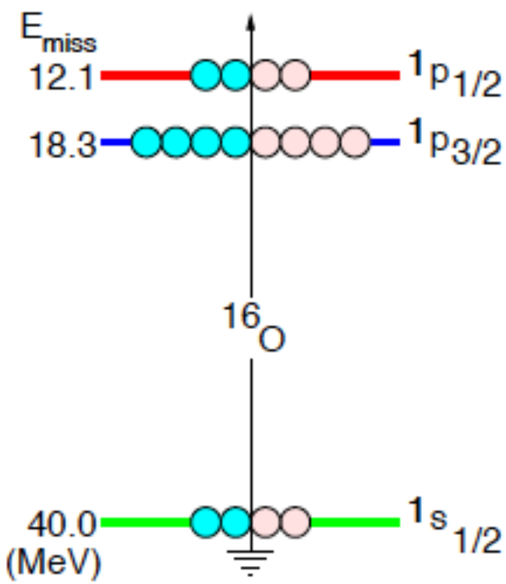

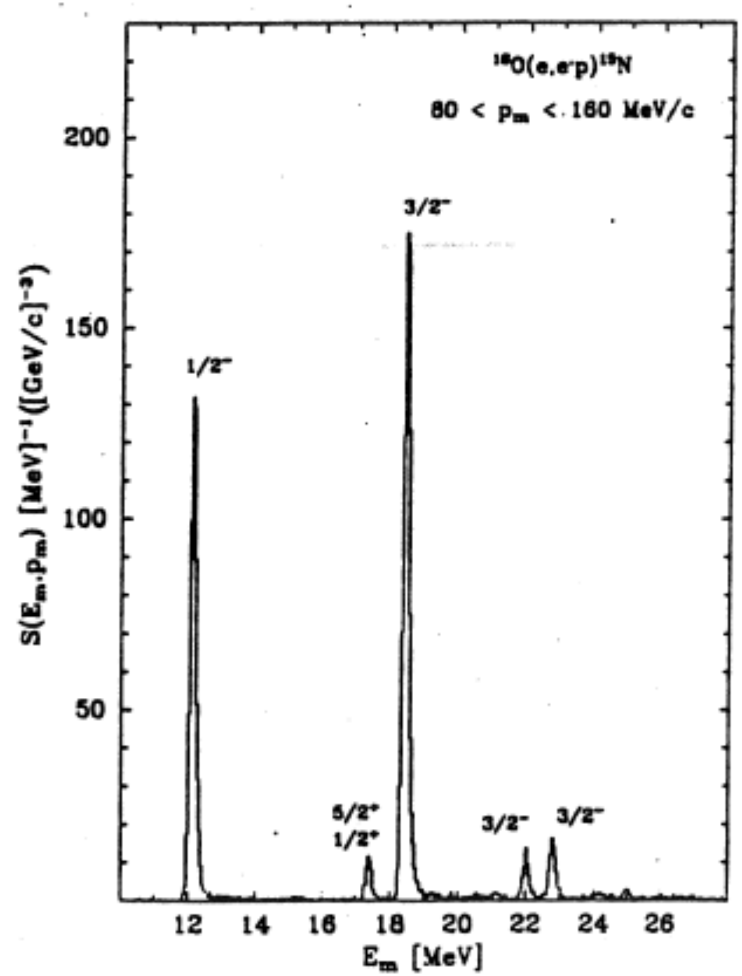

Neutrino Oscillations

- 2-Flavor Oscillation:

$$P(\nu_\mu \rightarrow \nu_e) = \sin^2 2\theta \sin^2 \left(\frac{\Delta m^2 L}{4 E_\nu} \right)$$

Know: L, need E_ν to determine Δm^2, θ

- 3-Flavor Oscillation: allows for CP violation

Observable Oscillation Parameters

$$P(\nu_\mu \to \nu_e) = \sin^2 2\theta \sin^2\left(\frac{\Delta m^2 L}{4E_\nu}\right)$$

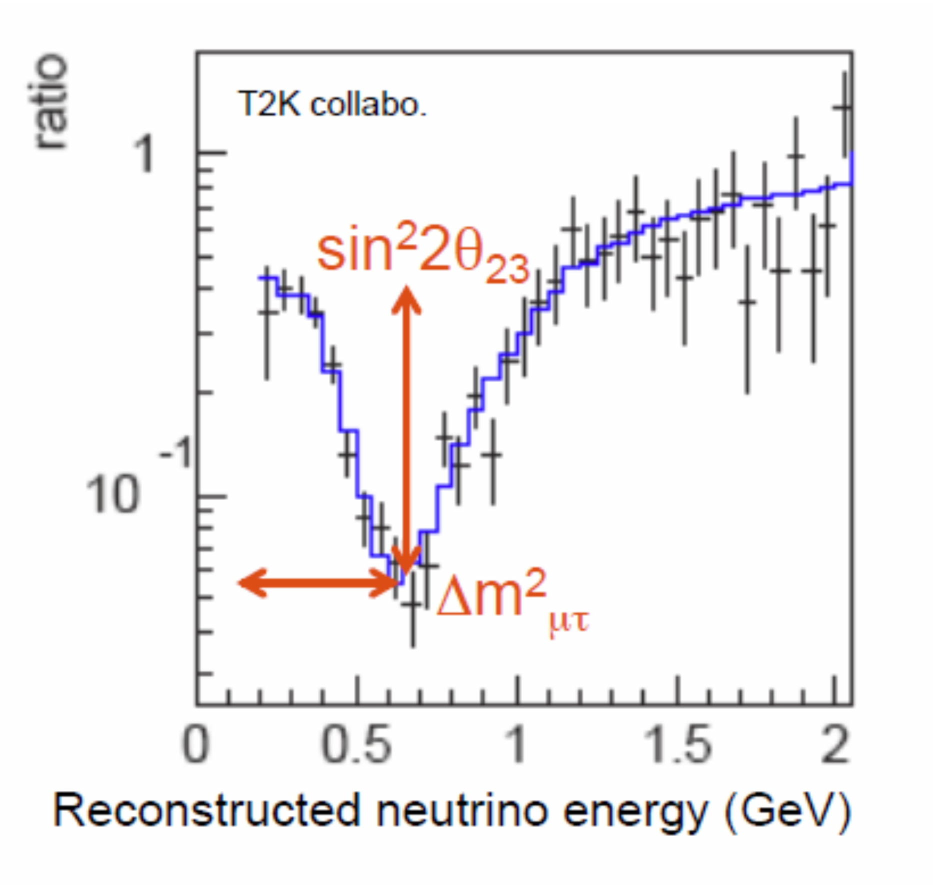

Oscillation probability

Long-Baseline Accelerator Appearance Experiments

- Oscillation probability complicated and dependent not only on θ_{13} but also:
  1. CP violation parameter (δ)
  2. Mass hierarchy (sign of Δm_{31}^2)
  3. Size of $\sin^2\theta_{23}$

$$
\begin{aligned}
P(\nu_\mu \to \nu_e) &= 4C_{13}^2 S_{13}^2 S_{23}^2 \sin^2 \frac{\Delta m_{31}^2 L}{4E} \times \left(1 + \frac{2a}{\Delta m_{31}^2} \ (1-2S_{13}^2)\right) \\
&+8C_{13}^2 S_{12} S_{13} S_{23} (C_{12} C_{23} \cos\delta - S_{12} S_{13} S_{23}) \cos \frac{\Delta m_{32}^2 L}{4E} \sin \frac{\Delta m_{31}^2 L}{4E} \sin \frac{\Delta m_{21}^2 L}{4E} \\
&-8C_{13}^2 C_{12} C_{23} S_{12} S_{13} S_{23} \sin\delta \sin \frac{\Delta m_{32}^2 L}{4E} \sin \frac{\Delta m_{31}^2 L}{4E} \sin \frac{\Delta m_{21}^2 L}{4E} \\
&+4S_{12}^2 C_{13}^2 \left\{C_{12}^2 C_{23}^2 + S_{12}^2 S_{23}^2 S_{13}^2 - 2C_{12} C_{23} S_{12} S_{23} S_{13} \cos\delta\right\} \sin^2 \frac{\Delta m_{21}^2 L}{4E} \\
&-8C_{13}^2 S_{13}^2 S_{23}^2 \cos \frac{\Delta m_{32}^2 L}{4E} \sin \frac{\Delta m_{31}^2 L}{4E} \frac{aL}{4E} \ (1-2S_{13}^2)
\end{aligned}
$$

⇒ These extra dependencies are both a "curse" and a "blessing"

Reactor Disappearance Experiments

$$P(\bar{\nu}_e \to \bar{\nu}_e) = 1 - \sin^2 2\theta_{13} \sin^2 \frac{\Delta m_{13}^2 L}{4E} + \ \textit{small terms}$$

Current Knowledge:

arXiv:1706.03621 [hep-ph]

	θ_{12}	θ_{13}	θ_{23}	$\Delta m^2_{21}/10^{-5}$	$\Delta m^2_{3j}/10^{-3}$	δ_{CP}
Normal Ordering	$33.56^{+0.77}_{-0.75}$	$8.46^{+0.15}_{-0.15}$	$41.6^{+1.5}_{-1.2}$	$7.50^{+0.19}_{-0.17}$	$2.524^{+0.039}_{-0.040}$	261^{+51}_{-59}
Inverted Ordering	$33.56^{+0.77}_{-0.75}$	$8.49^{+0.15}_{-0.15}$	$50.0^{+1.1}_{-1.4}$	$7.50^{+0.19}_{-0.17}$	$-2.514^{+0.038}_{-0.041}$	277^{+40}_{-46}

Current and Future Goals:

- Establish whether there is CP violation in the lepton sector and, if so, measure δ_{CP}
- Improve the accuracy on θ_{23}
- Determine the neutrino mass ordering: $m_1 < m_2 < m_3$ or $m_3 < m_1 < m_2$

Current and Future Experiments:

- **MiniBooNE** (concluded, re-running), **NOvA** (running), **T2K** (running), **T2HK** (under construction), etc.
- **SBN Program: MicroBooNE** (running), **ICARUS** (under construction), **SBND** (under construction)
- **DUNE** (under construction)

LArTPC (SBN Program and DUNE)

Current Knowledge:

arXiv: 1706.03621 [hep-ph]

	θ_{12}	θ_{13}	θ_{23}	$\Delta m^2_{21}/10^{-5}$	$\Delta m^2_{3j}/10^{-3}$	δ_{CP}
Normal Ordering	$33.56^{+0.77}_{-0.75}$	$8.46^{+0.15}_{-0.15}$	$41.6^{+1.5}_{-1.2}$	$7.50^{+0.19}_{-0.17}$	$2.524^{+0.039}_{-0.040}$	261^{+51}_{-59}
Inverted Ordering	$33.56^{+0.77}_{-0.75}$	$8.49^{+0.15}_{-0.15}$	$50.0^{+1.1}_{-1.4}$	$7.50^{+0.19}_{-0.17}$	$-2.514^{+0.038}_{-0.041}$	277^{+40}_{-46}

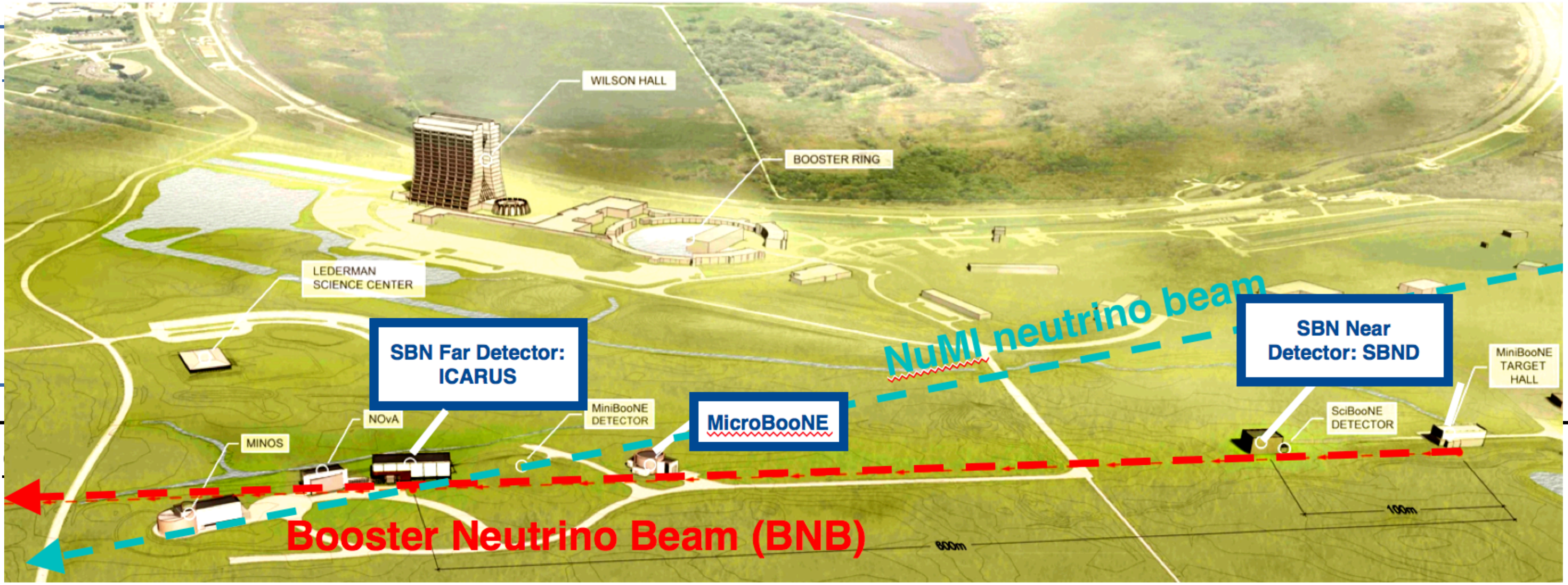

- **SBN Program: MicroBooNE** (running), **ICARUS** (under construction), **SBND** (under construction)
- **DUNE** (under construction)

LArTPC

Accelerator-based neutrino-oscillation experiments

DUNE

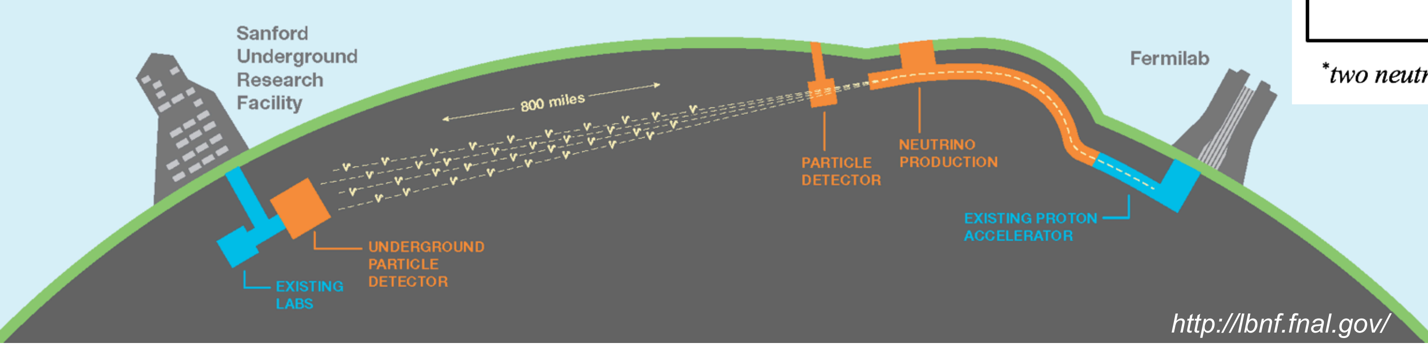

Oscillation Probability*:

$$P(\nu_\alpha \to \nu_\beta) \simeq \sin^2 2\theta \sin^2\left(\frac{\Delta m^2 L}{4E}\right)$$

**two neutrino flavors, for simplicity*

Experiments measure event rates which, for a given observable topology, can be naively computed as:

Event Rate at near detector:

$$N^{\alpha}_{\mathrm{ND}}(\boldsymbol{p}_{\mathrm{reco}}) = \sum_i \phi_\alpha(E_{\mathrm{true}}) \times \sigma^i_\alpha(\boldsymbol{p}_{\mathrm{true}}) \times \epsilon_\alpha(\boldsymbol{p}_{\mathrm{true}}) \times R_i(\boldsymbol{p}_{\mathrm{true}};\boldsymbol{p}_{\mathrm{reco}})$$

Event Rate at far detector:

$$N^{\alpha\to\beta}_{\mathrm{FD}}(\boldsymbol{p}_{\mathrm{reco}}) = \sum_i \phi_\alpha(E_{\mathrm{true}}) \times P_{\alpha\beta}(E_{\mathrm{true}}) \times \sigma^i_\beta(\boldsymbol{p}_{\mathrm{true}}) \times \epsilon_\beta(\boldsymbol{p}_{\mathrm{true}}) \times R_i(\boldsymbol{p}_{\mathrm{true}};\boldsymbol{p}_{\mathrm{reco}})$$

Event Rate at far detector:

$$N_{\rm FD}^{\alpha\to\beta}(\boldsymbol{p}_{\rm reco}) = \sum_i \phi_\alpha(E_{\rm true}) \times P_{\alpha\beta}(E_{\rm true}) \times \sigma_\beta^i(\boldsymbol{p}_{\rm true}) \times \epsilon_\beta(\boldsymbol{p}_{\rm true}) \times R_i(\boldsymbol{p}_{\rm true};\boldsymbol{p}_{\rm reco}):$$

$$P(\nu_\alpha \to \nu_\beta) \simeq \sin^2 2\theta \sin^2\left(\frac{\Delta m^2 L}{4E}\right)$$

Neutrino Energy: Reconstruction

Neutrino energy distribution

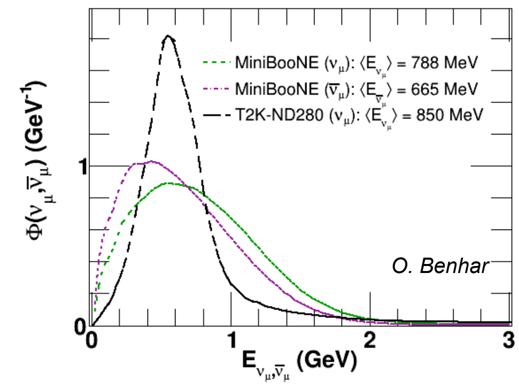

CCQE

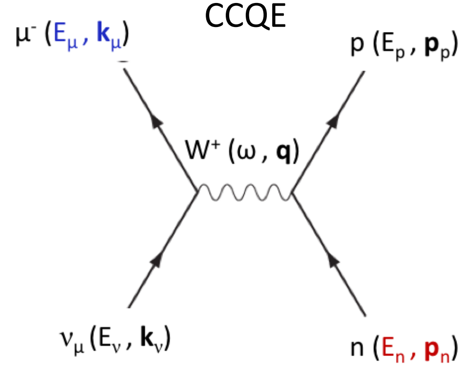

- For CCQE process (assuming single nucleon knock out), The reconstructed neutrino energy is

$$E_\nu = \frac{m_p^2 - m_\mu^2 - E_n{}^2 + 2E_\mu E_n - 2\mathbf{k}_\mu \cdot \mathbf{p}_n + |\mathbf{p}_n{}^2|}{2(E_n - E_\mu + |\mathbf{k}_\mu|\cos\theta_\mu - |\mathbf{p}_n|\cos\theta_n)}$$

where $|k_\mu|$ and θ_μ are measured, while p_n and E_n are the unknown momentum and energy of the interacting neutron.

- Existing simulation codes routinely use $|p_n| = 0$, $E_n = m_n - \varepsilon$, with $\varepsilon \sim 20$ MeV for carbon and oxygen, or the Fermi gas (FG) model.

Event Rate at far detector:

$$N_{FD}^{\alpha\to\beta}(\boldsymbol{p}_{reco}) = \sum_i \phi_\alpha(E_{true}) \times P_{\alpha\beta}(E_{true}) \times \sigma_\beta^i(\boldsymbol{p}_{true}) \times \epsilon_\beta(\boldsymbol{p}_{true}) \times R_i(\boldsymbol{p}_{true};\boldsymbol{p}_{reco})$$

$$P(\nu_\alpha \to \nu_\beta) \simeq \sin^2 2\theta \sin^2\left(\frac{\Delta m^2 L}{4E}\right)$$

Neutrino Energy: Reconstruction

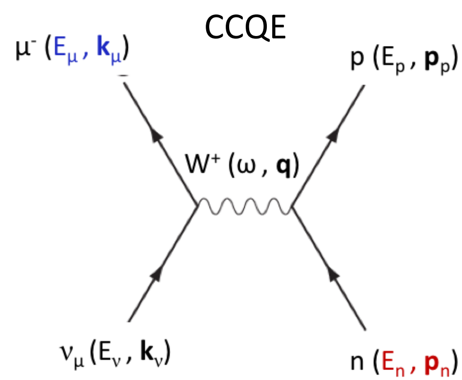

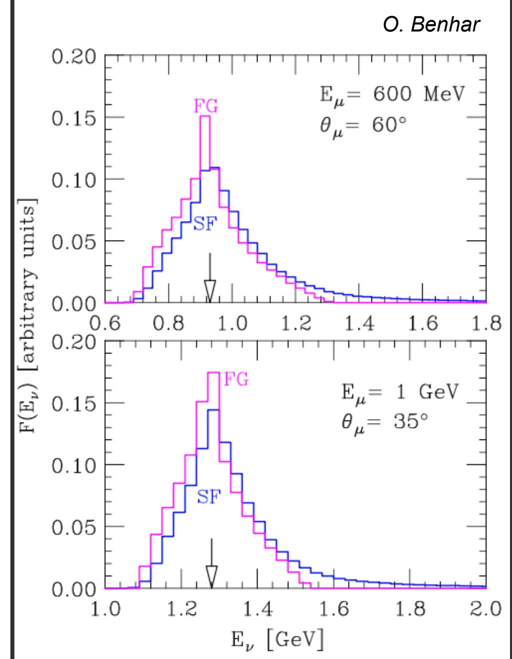

- For CCQE process (assuming single nucleon knock out), The reconstructed neutrino energy is

$$E_\nu = \frac{m_p^2 - m_\mu^2 - E_n{}^2 + 2E_\mu E_n - 2\mathbf{k}_\mu \cdot \mathbf{p}_n + |\mathbf{p}_n{}^2|}{2(E_n - E_\mu + |\mathbf{k}_\mu|\cos\theta_\mu - |\mathbf{p}_n|\cos\theta_n)}$$

- Neutrino energy reconstructed using 2 ×10^4 pairs of (|p|, E) values sampled from realistic (SF) and FG oxygen spectral functions.
- The average value $\langle E_\nu \rangle$ obtained from the realistic spectral function turns out to be shifted towards larger energy by ~ 70 MeV.

Event Rate at far detector:

$$N_{\rm FD}^{\alpha\to\beta}(\boldsymbol{p}_{\rm reco}) = \sum_i \phi_\alpha(E_{\rm true}) \times P_{\alpha\beta}(E_{\rm true}) \times \sigma_\beta^i(\boldsymbol{p}_{\rm true}) \times \epsilon_\beta(\boldsymbol{p}_{\rm true}) \times R_i(\boldsymbol{p}_{\rm true};\boldsymbol{p}_{\rm reco});$$

Neutrino-nucleus cross section

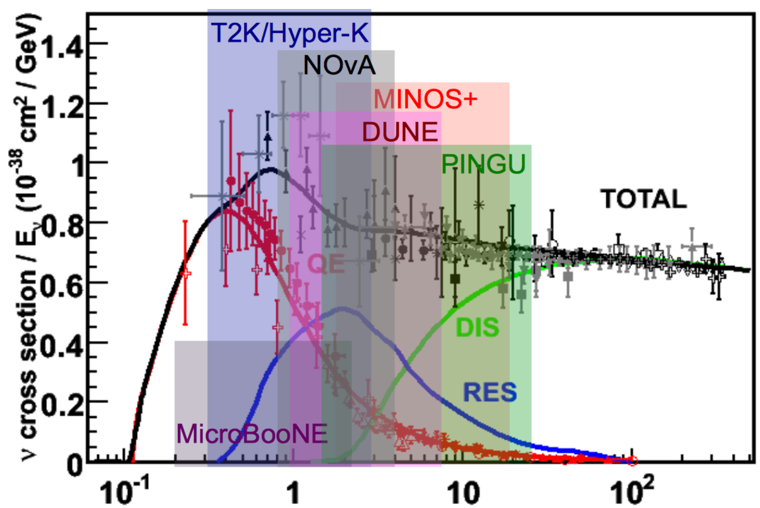

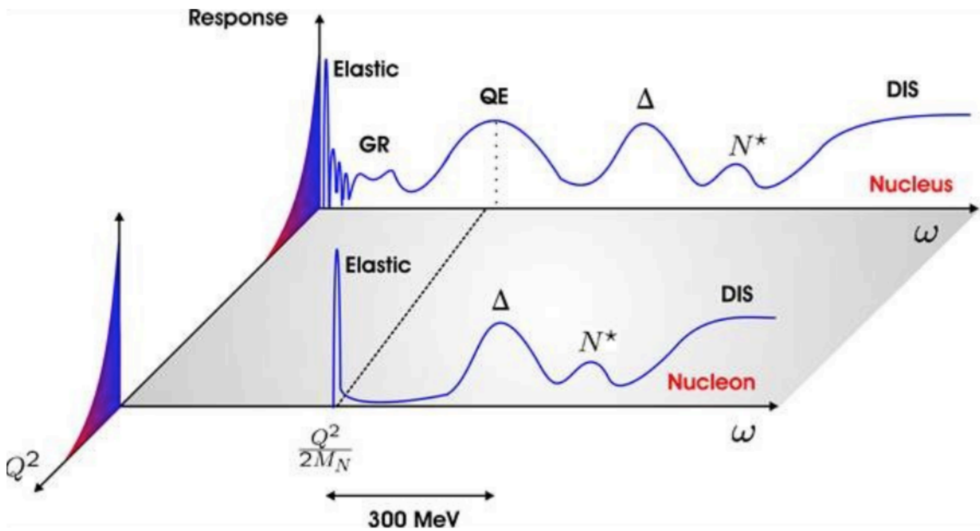

- Need realistic nuclear model (in Monte-Carlo simulations) that can describe neutrino-nucleus cross sections over a wide range of energies.

Appearance Probability as function of neutrino energy

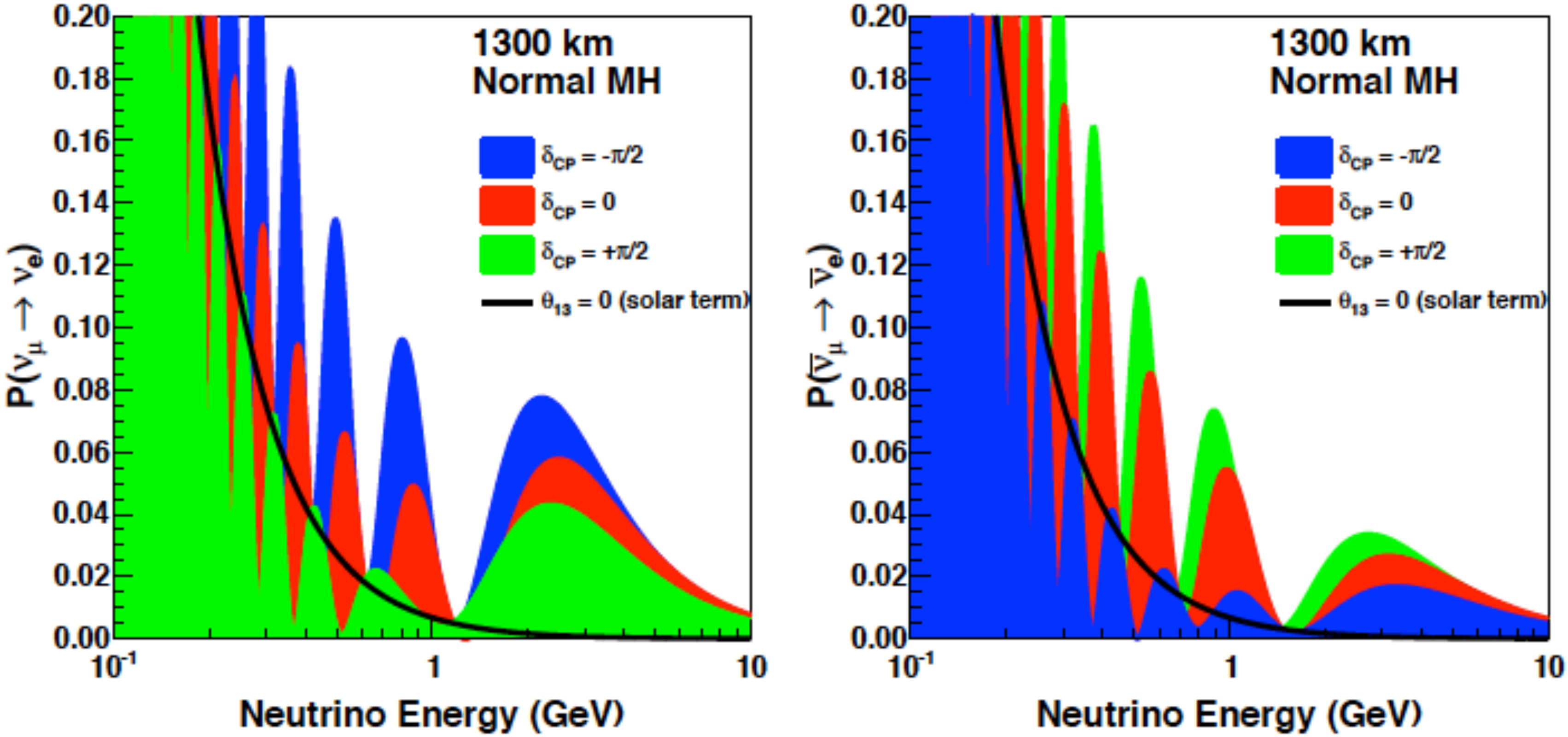

Need energy to distinguish between different δ_{CP}

Effect of an underestimation of the missing energy in the calorimetric energy reconstruction on the coincidence regions in the θ_{13},δ plane.

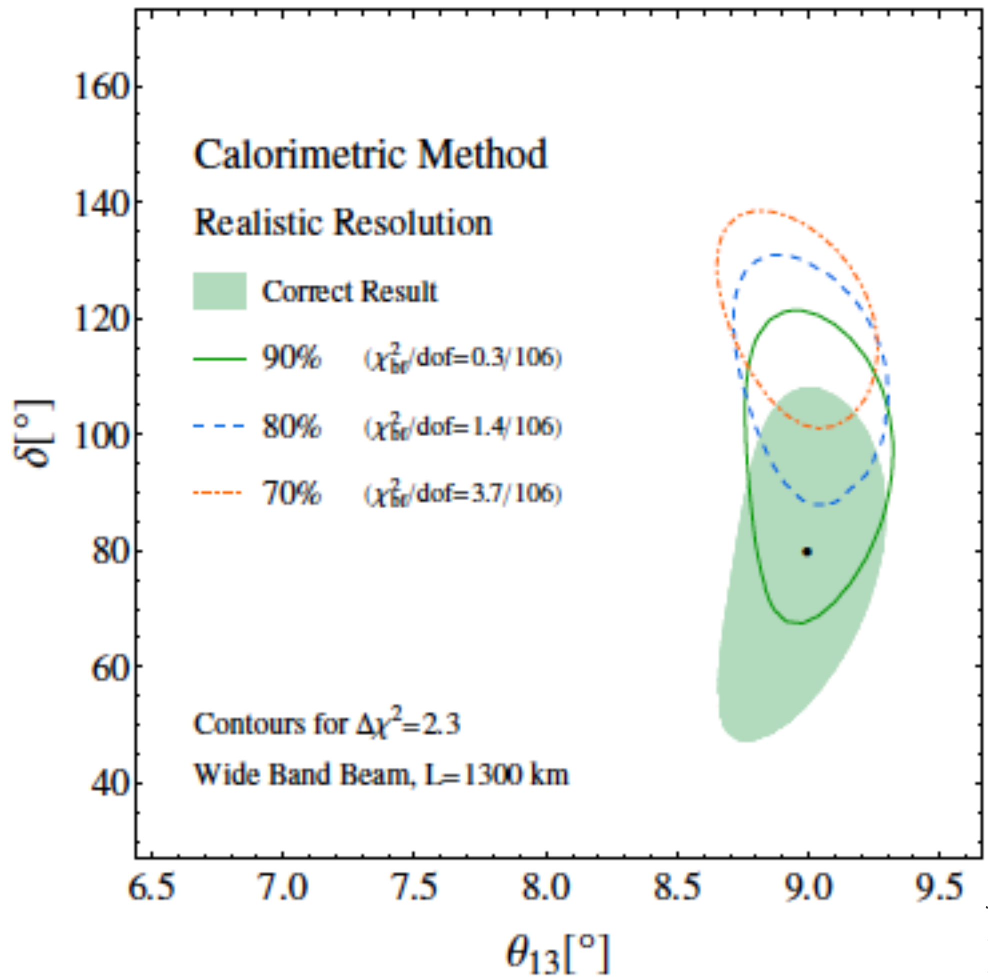

J.Phys.G, Nucl.Part.Phys. 44 (2017), 054001
Physics Report 700 (2017) 1
PRD D92, 091301 (2015) - arxiv: 1507.08560

Expected sensitivity of DUNE to CP violation as a function of exposure in kt·MW·year for a range of values for the ν_e and $\bar{\nu}_e$ signal normalization uncertainties from $5\% \oplus 3\%$ to $5\% \oplus 1\%$.

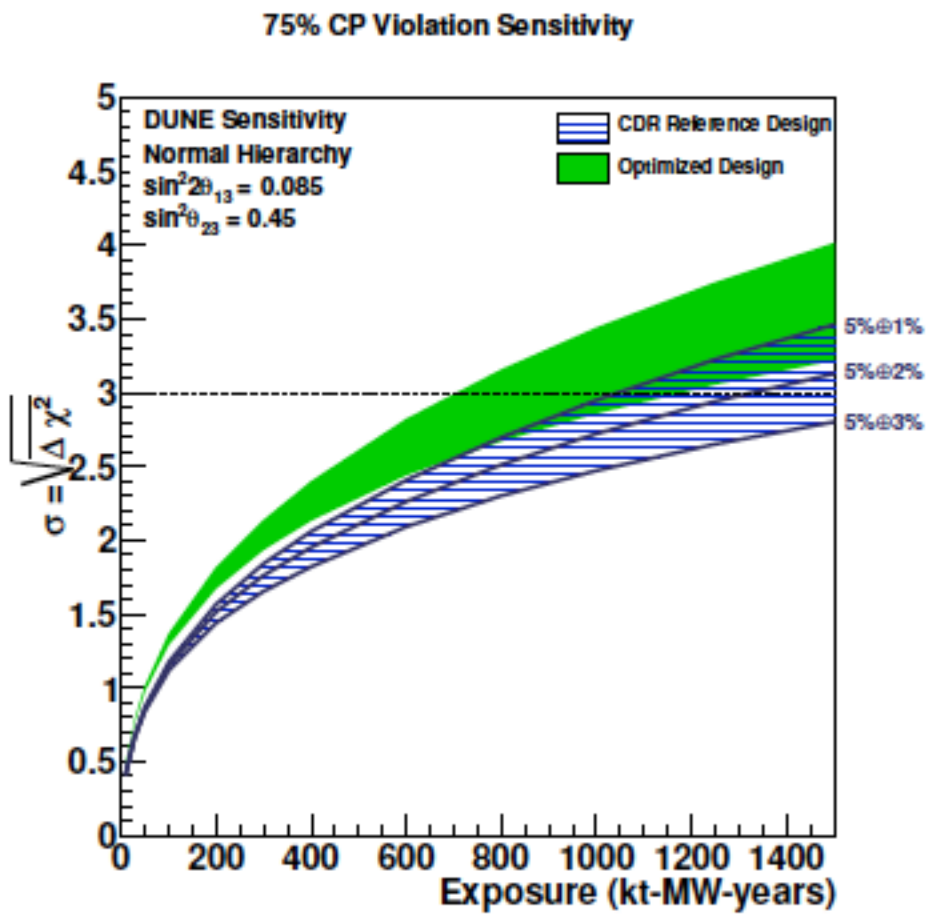

Oscillation Signal: Dependence on Hierarchy and Mixing Angle

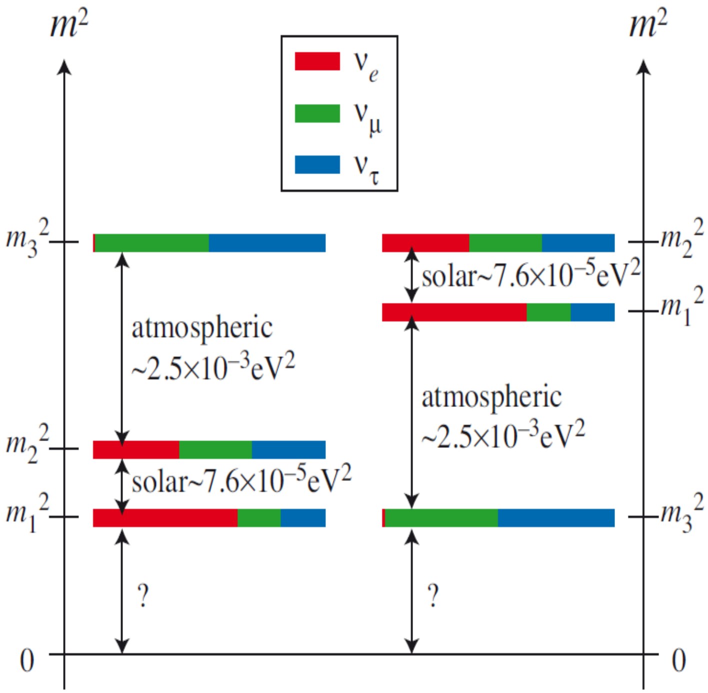

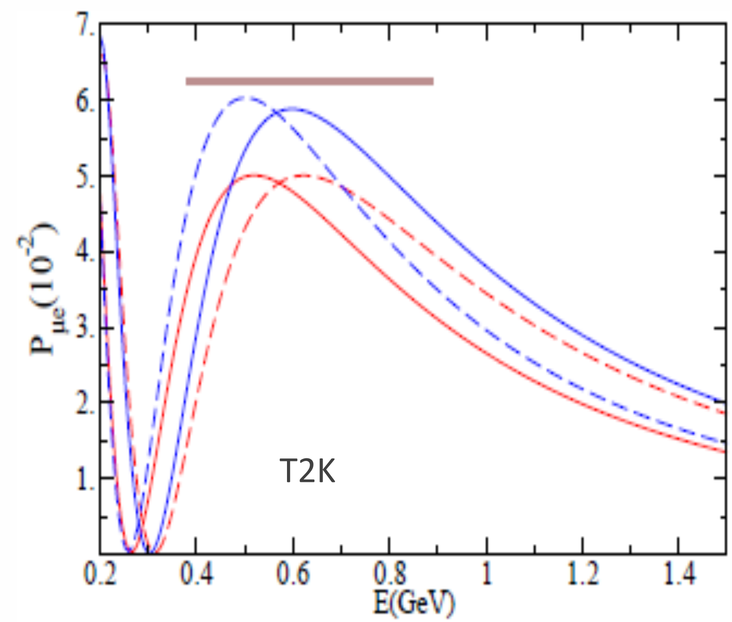

Fig. 2. $\mathcal{P}_{\mu e}$ in matter versus neutrino energy for the T2K experiment. The blue curves depict the normal hierarchy, red the inverse hierarchy. Solid curves depict positive θ_{13}, dashed curves negative θ_{13}

D.J. Ernst et al.,

Energy has to be known better than 50 MeV

Shape sensitive to hierarchy and sign of mixing angle

Appearance experiment

- Near detector:
  - Neutrino Flux
  - Background
  - Intrinsic ν_e
  - Neutrino energy

→

- Far detector:
  - Extrapolate Flux
  - Background
  - Neutrino energy

$$P(\nu_\mu \to \nu_e) = 1 - \sin^2 2\theta_{13} \sin^2\left(\frac{1.27\Delta m^2 L}{E_\nu}\right) + other$$

Neutrino Beams

- Neutrinos do not have fixed energy nor just one reaction mechanism

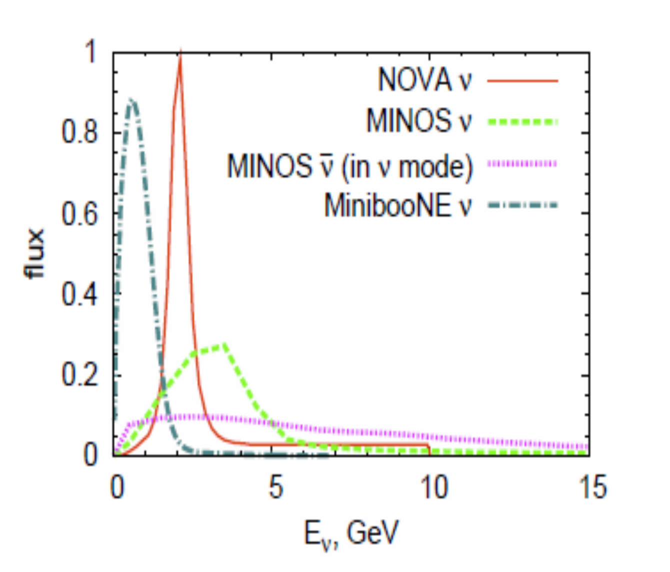

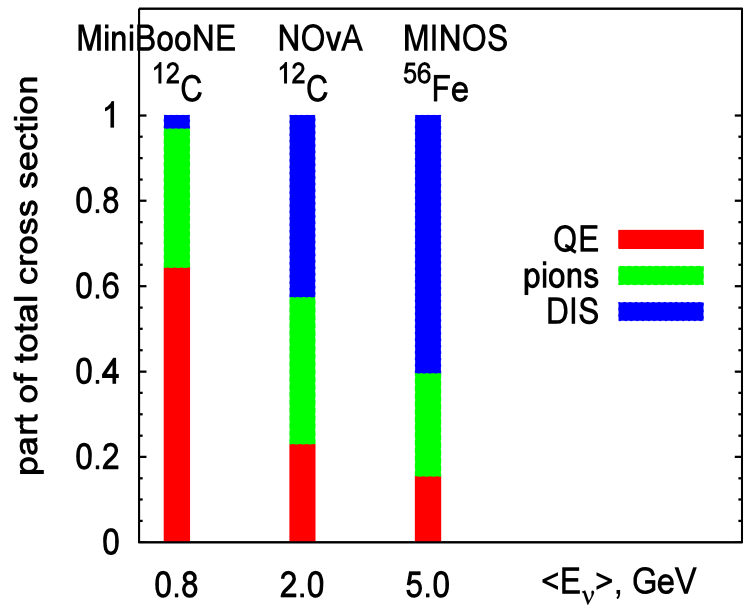

Have to reconstruct energy from final state of reaction
Different processes are entangled

Neutrino Interactions

- for ν_e appearance
  - -beam ν_e
  - -NCπ^0 events

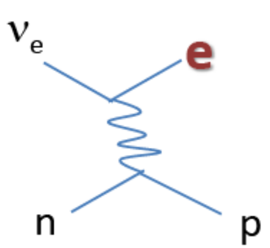

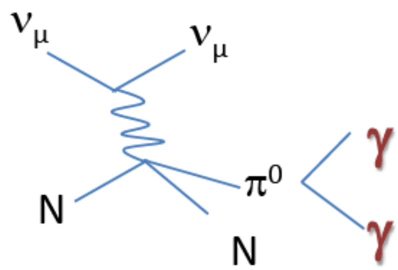

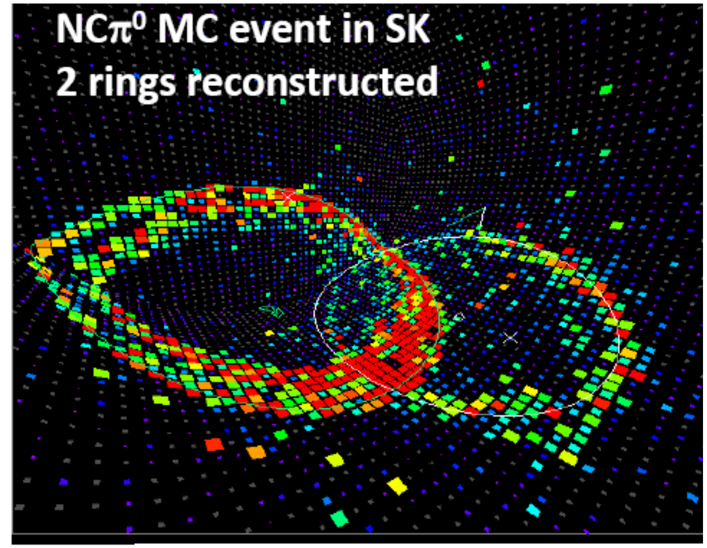

- for ν_μ disappearance (muon energy measurement)
  - -inelastic processes

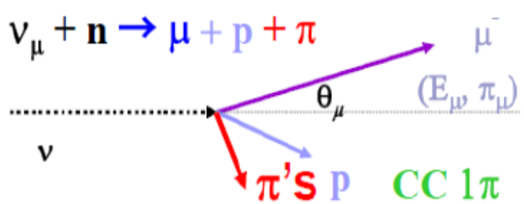

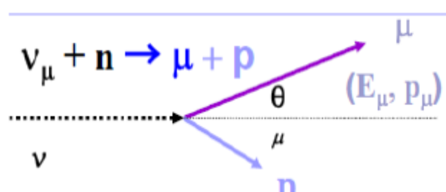

Quasi-Elastic process

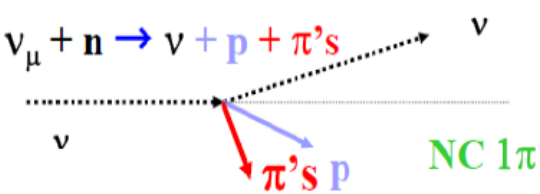

Energy reconstruction

$$\nu_\mu + n \rightarrow \mu^- + p$$

$$E_\nu = E_\nu(E_\mu, \theta_\mu)$$

Kinematic:

- Rely on underlying interaction to use relate outgoing lepton kinematics to neutrino energy
- Advantage:
  - don't need hadron reconstruction
- Disadvantages
  - energy is wrong if underlying interaction is wrong (i.e. not CCQE)
  - Nuclear effects smear resolution

$$\nu_\mu + N \rightarrow \mu^- + X$$

$$E_\nu = E_\mu + E_X$$

Calorimetric

- Add up the energy from the leptonic and hadronic components
- Advantages
  - No *a priori* assumption about underlying interaction
- Disadvantages
  - Relies on hadron reconstruction

Background: Nuclear re-interactions

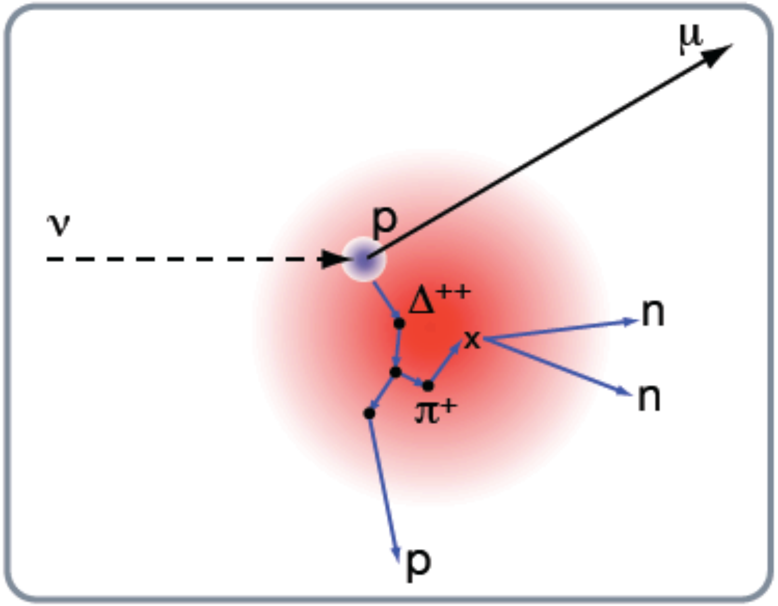

- Lepton kinematics shifted/smeared
- Outgoing hadronic final state ("topology") may differ from expectation from "underlying" ν-nucleon interaction
- FSI effects may appear degenerate with hadronic interactions outside of the target nucleus.

Modeling ν interactions in nucleus

- Underlying ν-nucleon/quark interaction
  - Mode (CCQE, resonance, etc.)
  - Determine "final" state of interaction
- Initial state nucleon/quark
  - Fermi motion, binding energy
- Final state effects
  - Pauli blocking
  - Propagate hadrons within nucleus
    - Absorption, scattering, CEX, etc.

How to quantify effects on oscillation

- Ideal, perfect near detector (^{12}C), 1 km, 1kton
- Far detector at 295 km, 22.5 kton, Carbon (SF)
- Use flux that peak at 0.6 GeV, 750kW, 5 years running
- Use a second flux that peaks at 1.5 GeV, 750kW, 5 years running
- Use Super Kamiokande (water cherenkov detector) reconstruction efficiency as function of energy
- Use migration matrices to take into account how neutrino energy reconstruction is affected by the what kind of interaction the neutrino undergo in the detector and how well we can identify them
- Muon neutrino disappearance only -> fit to atmospheric parameters

J.Phys.G, Nucl.Part.Phys. 44 (2017), 054001
Physics Report 700 (2017) 1

How to read the plots in the following slides

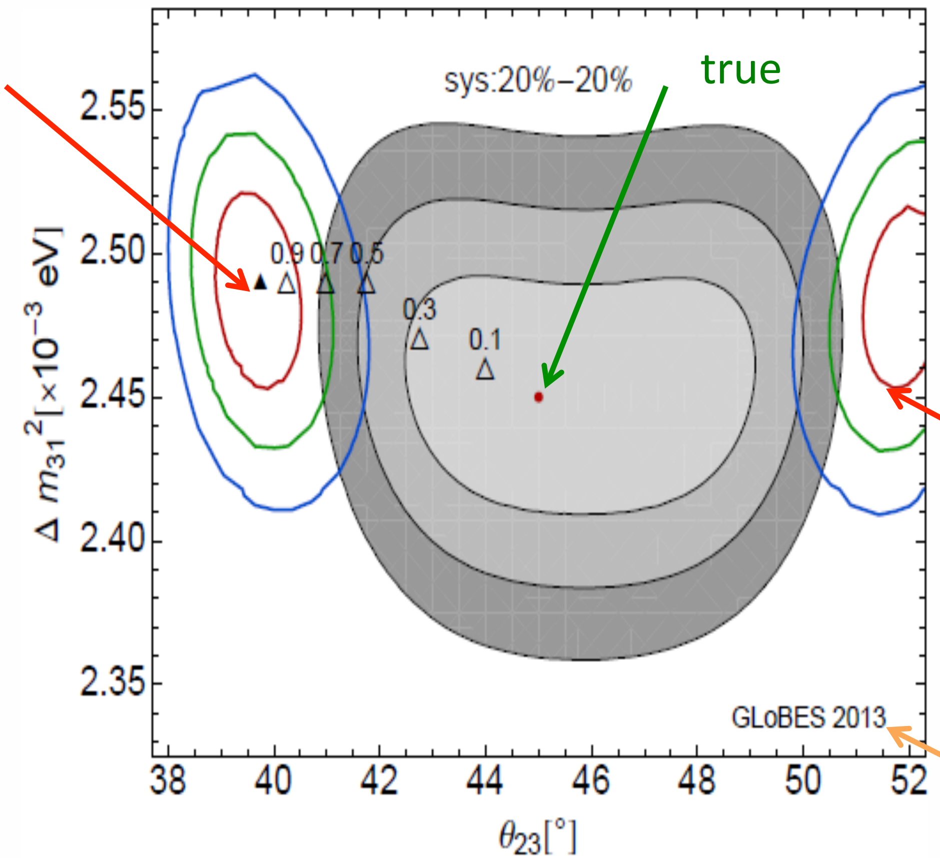

Dependence from target material (C vs O)

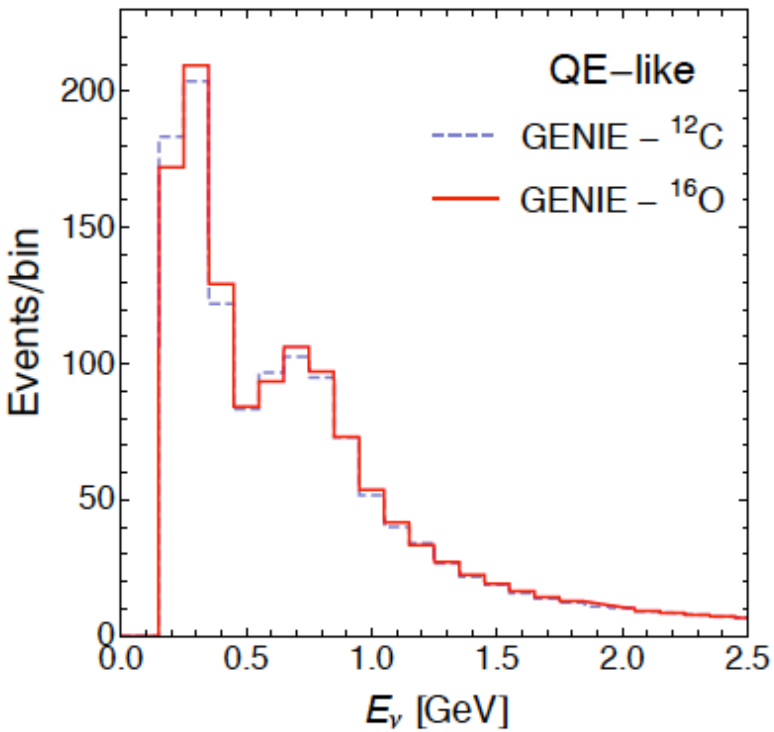

PRD D89, 073015 (2014) - arxiv:1311.4506

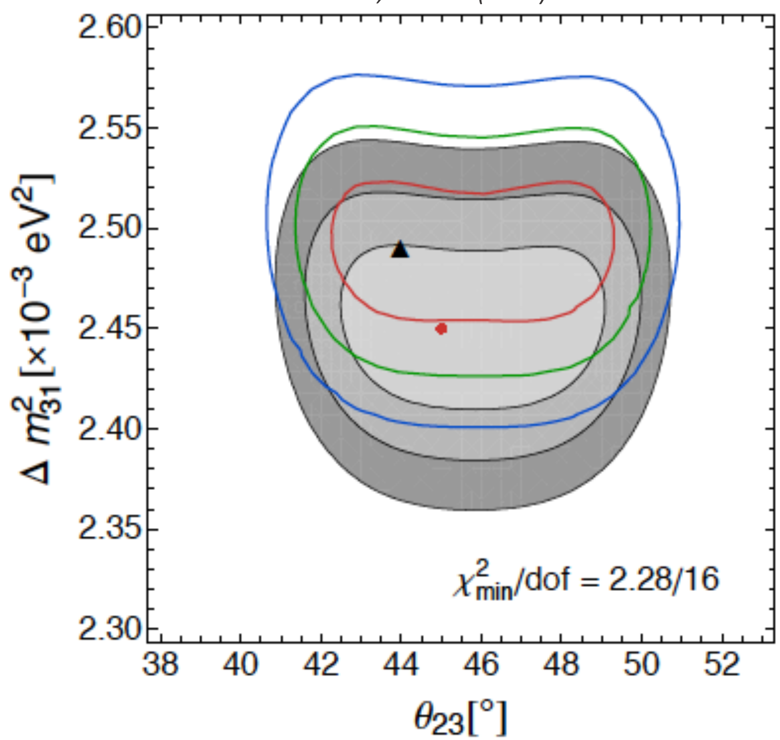

Dependence from nuclear model (1p1h)

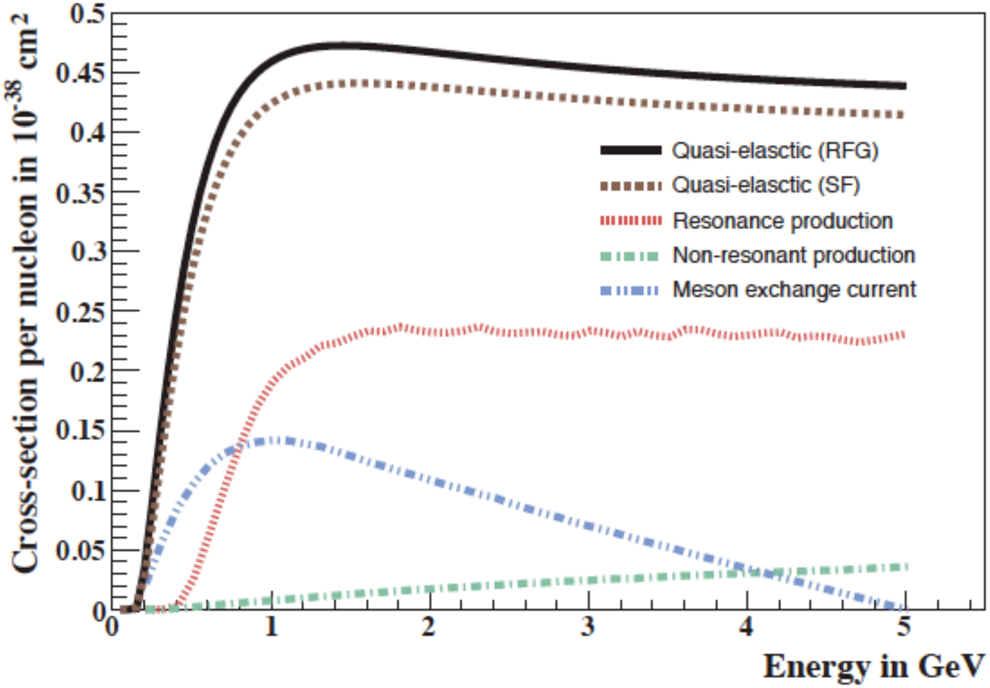

PRD D89, 093004 (2014) - arxiv:1402.6651

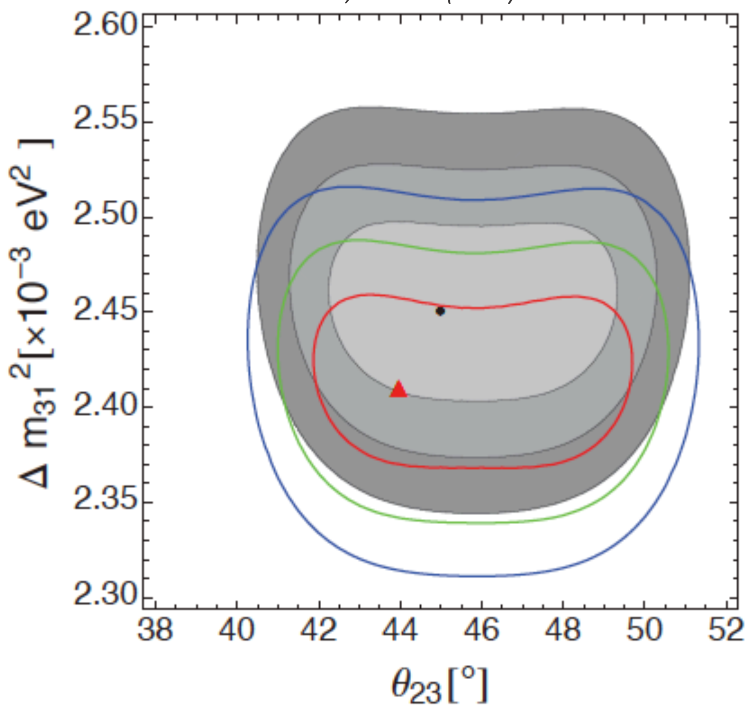

Dependence from nuclear model (2p2h)

PRD D93, 113004 (2016) - arxiv:1603.01072

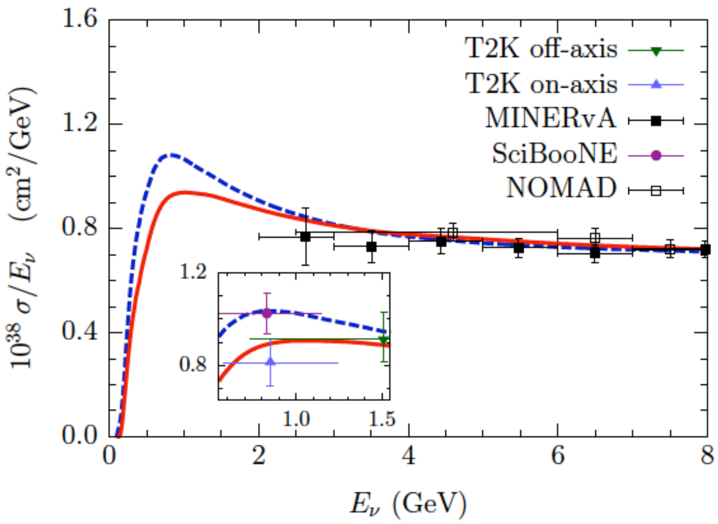

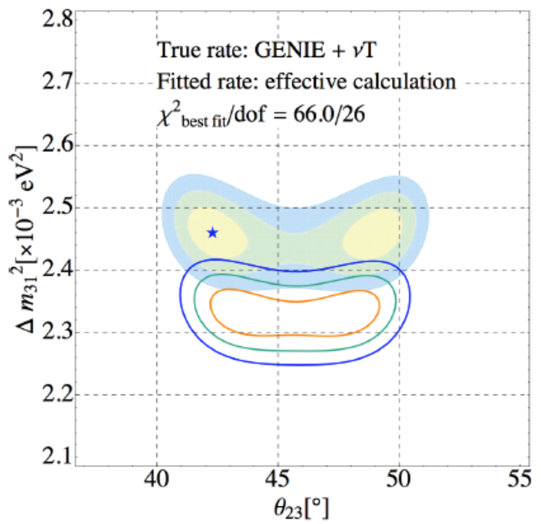

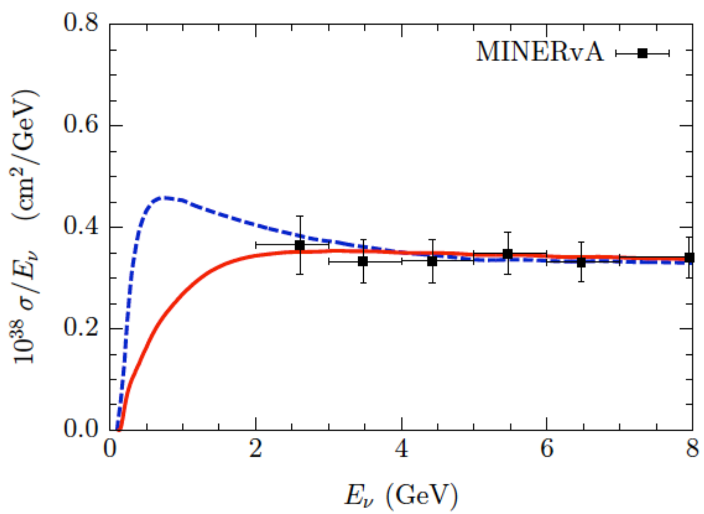

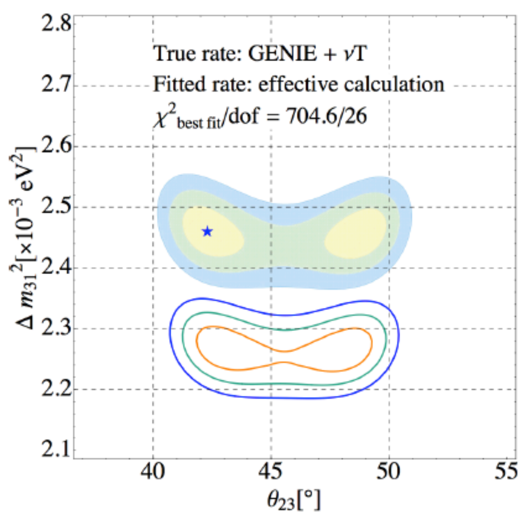

Two ways to reconstruct the neutrino energy

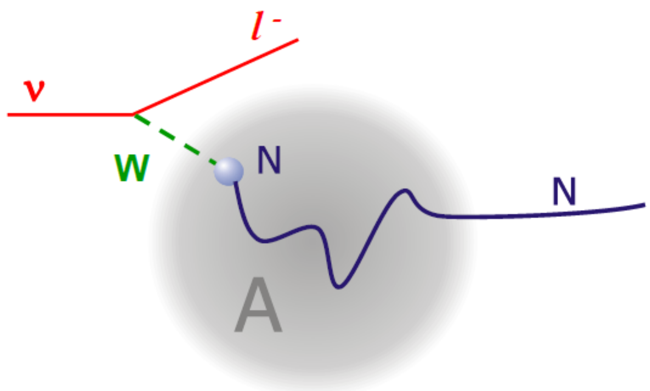

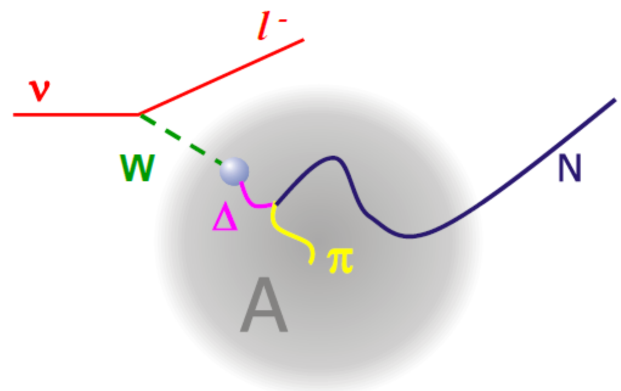

- Kinematic: use only info on the outgoing lepton kinematic
- Calorimetric: sum all energy in final state

Simulating a non perfect detector

- Detection thresholds
  - 20 MeV for mesons,
  - 40 MeV for protons

- Efficiencies
  - 60% for π^0,
  - 80% for other mesons,
  - 50% for protons,
  - *neutrons undetected*

$$\sigma(|\mathbf{k}_\mu|) = 0.02|\mathbf{k}_\mu| \quad \text{and} \quad \sigma(\theta) = 0.7^\circ$$

$$\frac{\sigma(E_{\pi^0})}{E_{\pi^0}} = \max\left\{\frac{0.107}{\sqrt{E_{\pi^0}}}, \frac{0.02}{E_{\pi^0}}\right\} \text{ and } \frac{\sigma(E_h)}{E_h} = \max\left\{\frac{0.145}{\sqrt{E_h}}, 0.067\right\}$$

Detector effects on kinematic energy reconstruction

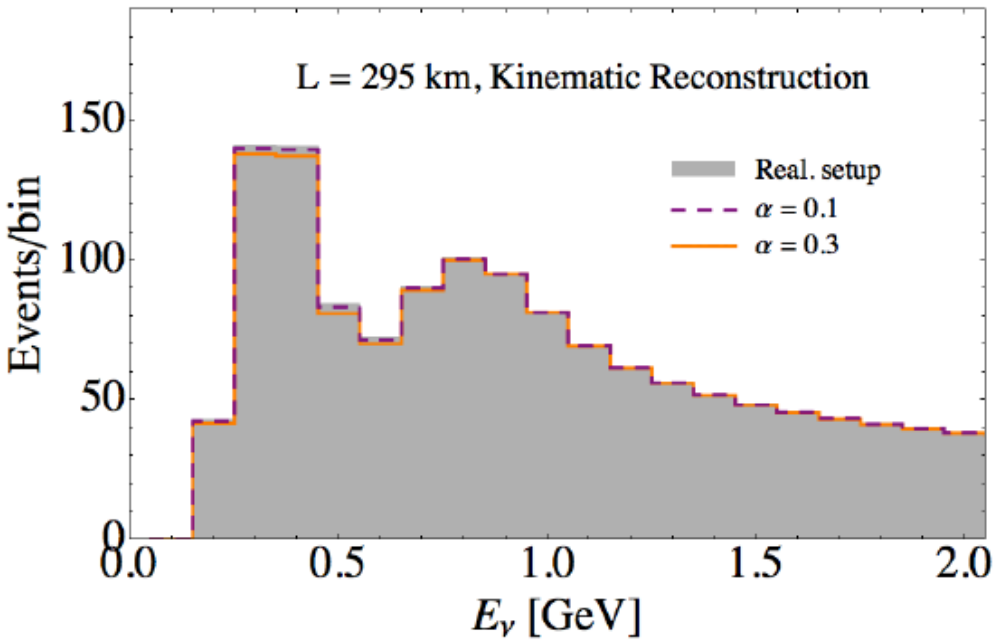

PRD D92, 091301 (2015) - arxiv:1507.08561

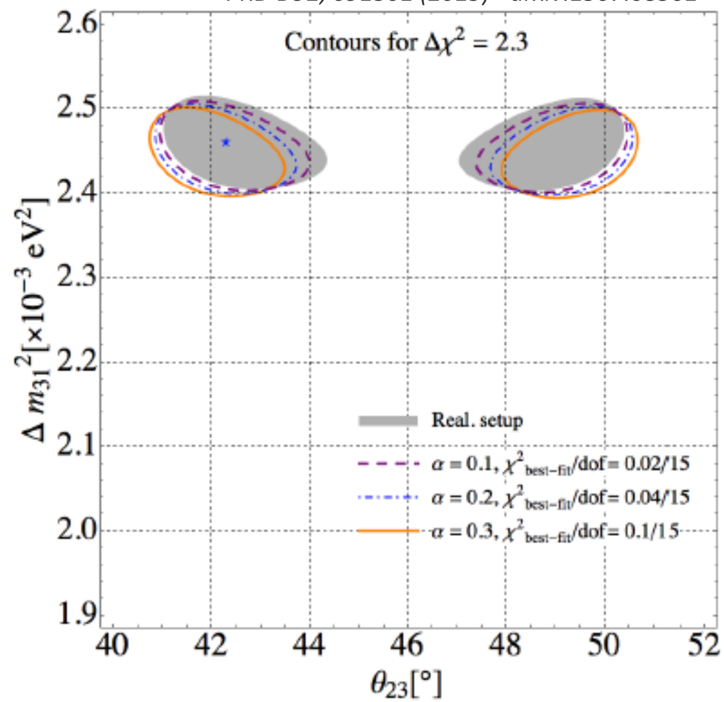

Detector effects on calorimetric energy reconstruction

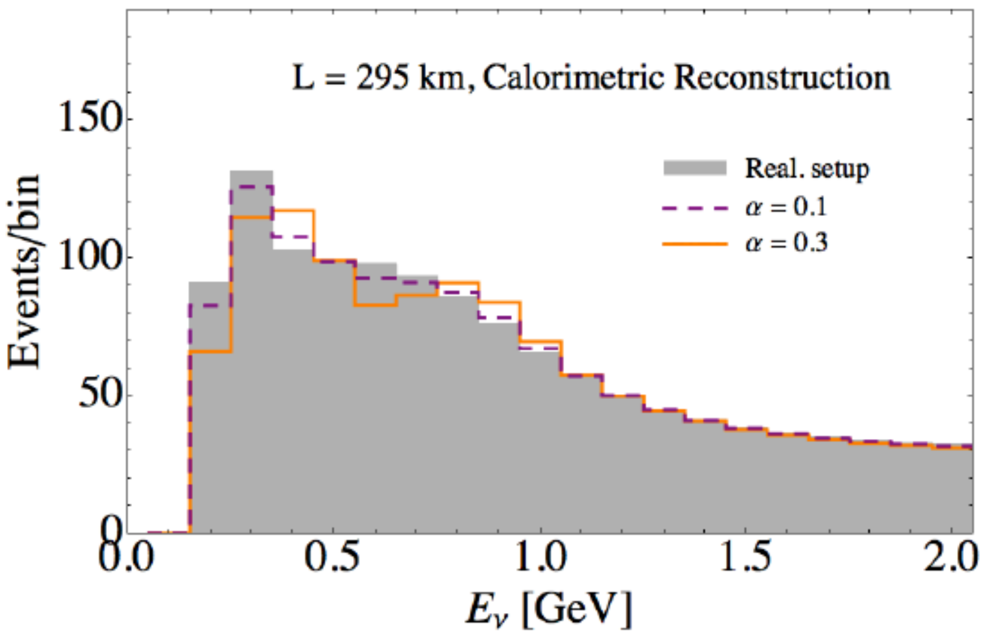

PRD D92, 091301 (2015) - arxiv:1507.08561

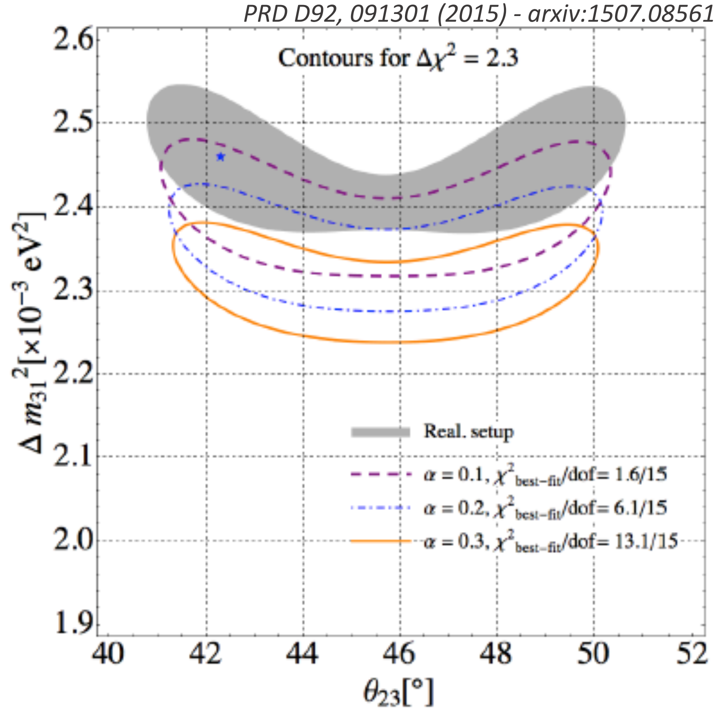

Electron vs neutrino scattering

QE e-A scattering

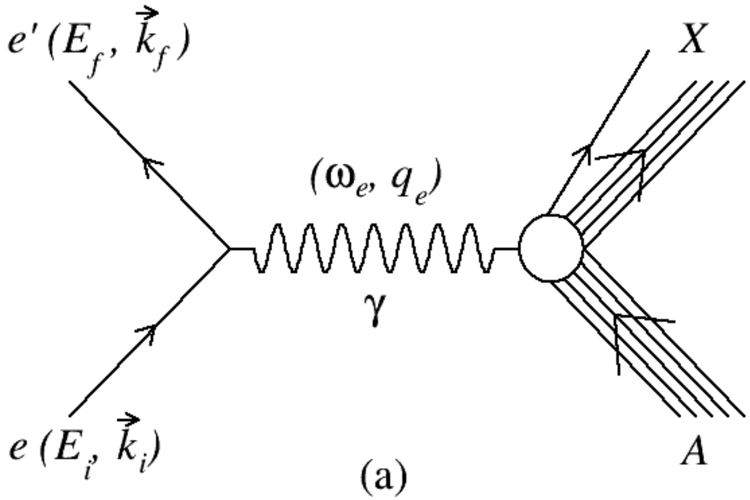

$$\left(\frac{d^2\sigma}{d\omega_e d\Omega}\right)_e = \frac{\alpha^2}{Q^4}\left(\frac{2}{2J_i+1}\right)\frac{1}{k_f E_i} \times \zeta^2(Z', E_f, q_e)\left[\sum_{J=0}^{\infty}\sigma^J_{L,e} + \sum_{J=1}^{\infty}\sigma^J_{T,e}\right]$$

$$\sigma_{L,e} = v_e^L R_e^L$$

$$\sigma_{T,e} = v_e^T R_e^T$$

v's → Leptonic coefficients → Purely kinematical → Easy to calculate

QE e-A scattering

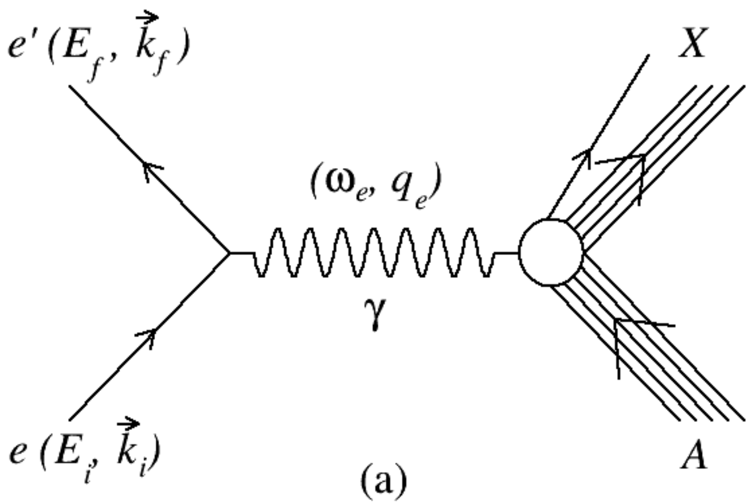

QE ν-A scattering

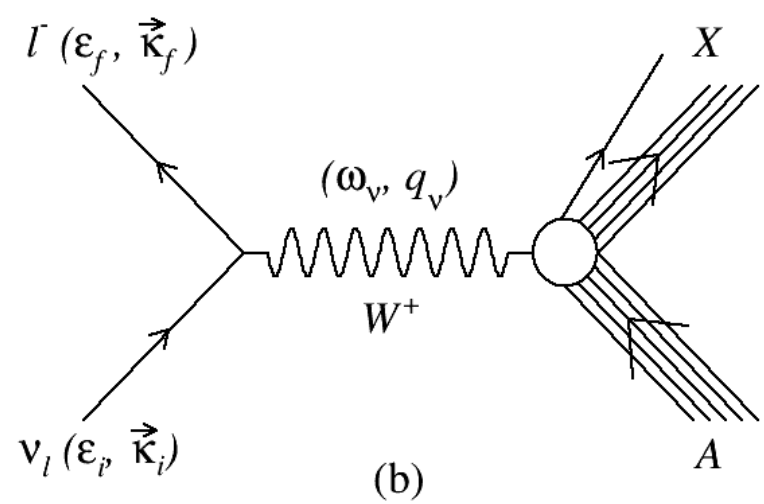

$$\left(\frac{d^2\sigma}{d\omega_e d\Omega}\right)_e = \frac{\alpha^2}{Q^4}\left(\frac{2}{2J_i+1}\right)\frac{1}{k_f E_i} \times \zeta^2(Z', E_f, q_e)\left[\sum_{J=0}^{\infty}\sigma^J_{L,e} + \sum_{J=1}^{\infty}\sigma^J_{T,e}\right]$$

$$\left(\frac{d^2\sigma}{d\omega_\nu d\Omega}\right)_\nu = \frac{G_F^2 \cos^2\theta_c}{(4\pi)^2}\left(\frac{2}{2J_i+1}\right)\varepsilon_f\kappa_f \times \zeta^2(Z', \varepsilon_f, q_\nu)\left[\sum_{J=0}^{\infty}\sigma^J_{CL,\nu} + \sum_{J=1}^{\infty}\sigma^J_{T,\nu}\right]$$

$$\sigma_{L,e} = v_e^L R_e^L$$

$$\sigma_{T,e} = v_e^T R_e^T$$

$$\sigma^J_{CL,\nu} = \left[v_\nu^{\mathcal{M}} R_\nu^{\mathcal{M}} + v_\nu^{\mathcal{L}} R_\nu^{\mathcal{L}} + 2\, v_\nu^{\mathcal{ML}} R_\nu^{\mathcal{ML}}\right]$$

$$\sigma^J_{T,\nu} = \left[v_\nu^T R_\nu^T \mp 2\, v_\nu^{TT} R_\nu^{TT}\right]$$

v's → Leptonic coefficients → Purely kinematical → Easy to calculate

R's → Response functions → Nuclear dynamics → **Need nuclear models to calculate!**

Electron scattering data as a validation

Longitudinal (left) and transverse (right) electromagnetic responses of ^{12}C at |q| = 570 MeV, as function of energy transfer

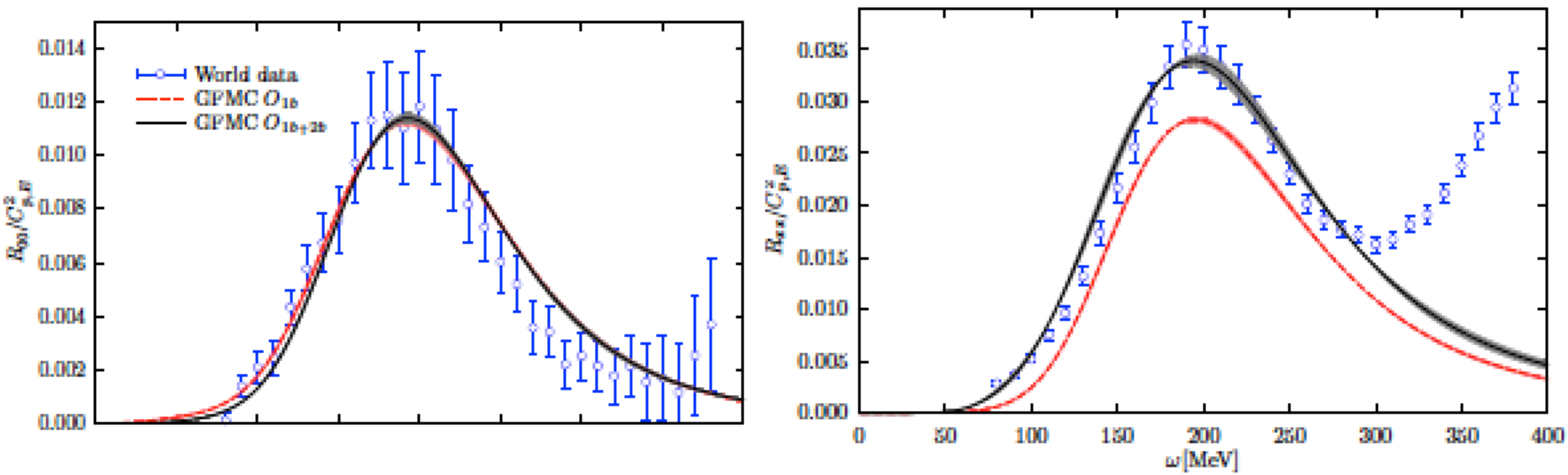

Theoretical results obtained using the Green's Function Monte Carlo (GFMC) technique, a realistic nuclear Hamiltonian and consistent one- and two-nucleon currents.

Note that, even at moderate momentum transfer, the non relativistic approach fails to describe the transverse response in the region of large energy transfer, where the contribution of inelastic processes is large.

Electron scattering data as a validation

$e + {}^{12}\mathrm{C} \rightarrow e' + X$ quasi elastic cross section computed within the IA including FSI. The predictions of the Relativistic Fermi Gas Model (RFGM) are also shown for comparison.

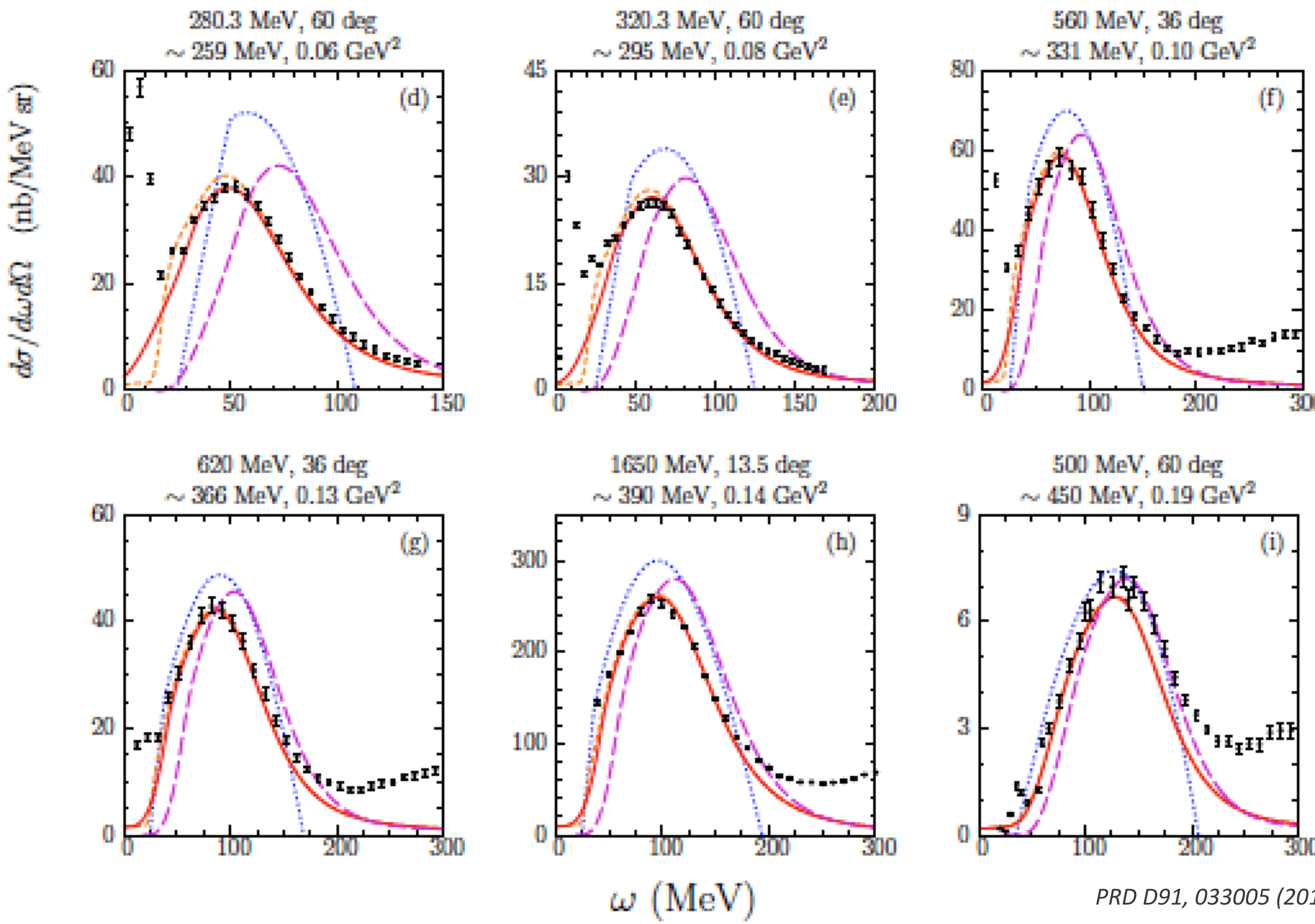

PRD D91, 033005 (2015) - arxiv:1404.5687

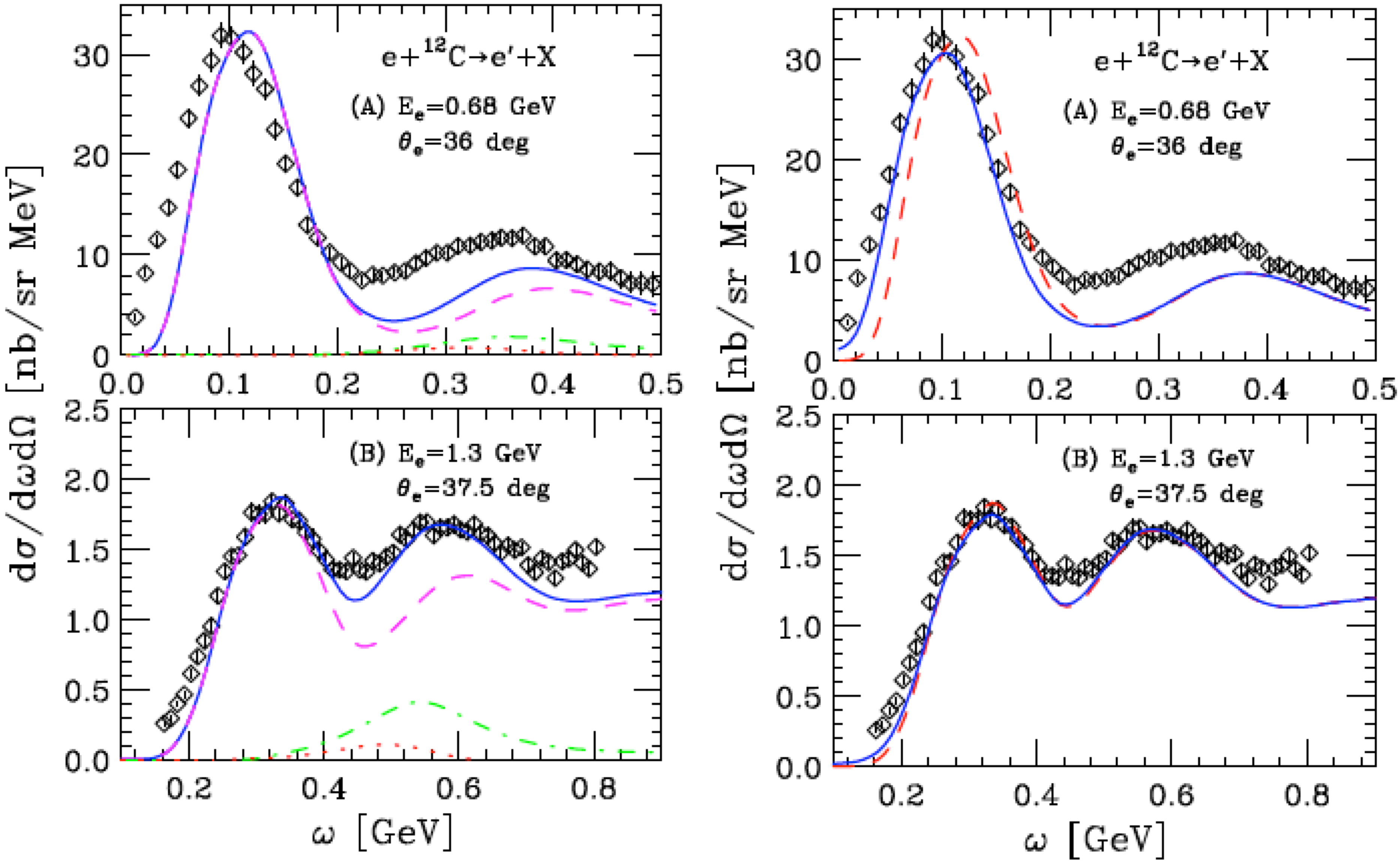

PRL 116, 192501 (2016) - arxiv:1512.07426

E12-14-012 at JLab

E12-14-012 Experiment

- **<u>Primary Goal</u>: Measurement of the spectral functions of argon nucleus** through (e,e'p) reaction

- Nevertheless, a new high precision e-Ar data will provide vital information about argon nucleus and it's electroweak interaction to the community that can be used as a testbed for the development of theoretical models/frameworks. And will be a significant step ahead in improving the accuracy of the measurement of the neutrino-oscillation parameters, more importantly the CP violation phase in leptonic sector.

Extracting Spectral Function from Data

- We plan to study the **coincidence (e,e'p) processes** in the **kinematical region** in which single nucleon knock out of a nucleon occupying a shell model orbit is the dominant reaction mechanism.

Coincidence *(e,e'p)* process:

- Both the outgoing electron and the proton are detected in coincidence, and the recoiling nucleus can be left in any bound state.

- Within the Plane Wave Impulse Approximation (PWIA) scheme:

$$\frac{d\sigma_A}{dE_{e'}d\Omega_{e'}dE_p d\Omega_p} \propto \sigma_{ep} P(p_m, E_m)$$

- The initial energy and momentum of the knocked out nucleon can be identified with the measured missing momentum and energy, respectively as

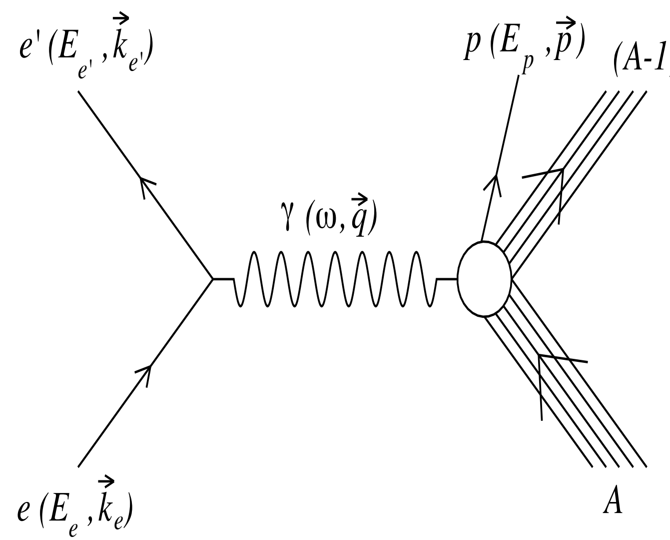

$$\mathbf{p}_m = \mathbf{p} - \mathbf{q}$$

$$E_m = \omega - T_p - T_{A-1} \sim \omega - T_p$$

Where $T_p = E_p - m$, is the kinetic energy of the outgoing proton.

Extracting Spectral Function from Data

<u>Kinematic region</u>:

- Separation energies of the proton and neutron shell model states for Ca (measured) and Ar ground states (predicted)

	protons		neutrons	
	$^{40}_{20}$Ca	$^{40}_{18}$Ar	$^{40}_{20}$Ca	$^{40}_{18}$Ar
$1s_{1/2}$	57.38	52	66.12	62
$1p_{3/2}$	36.52	32	43.80	40
$1p_{1/2}$	31.62	28	39.12	35
$1d_{5/2}$	14.95	11	22.48	18
$2s_{1/2}$	10.67	8	17.53	13.15
$1d_{3/2}$	8.88	6	15.79	11.45
$1f_{7/2}$				5.56

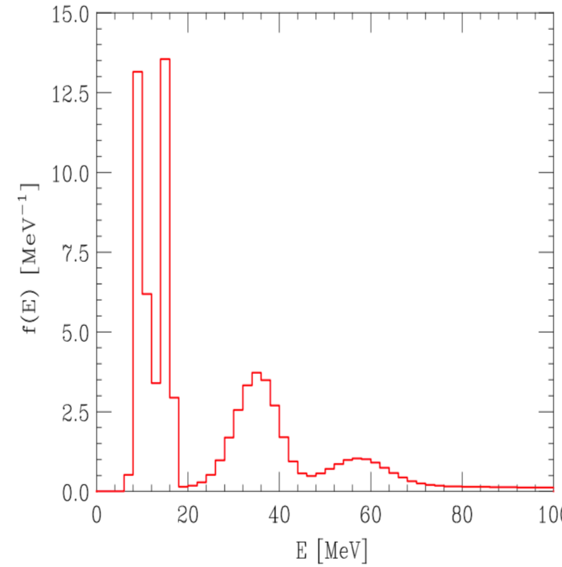

- The energy distribution

$$f(E) = 4\pi \int dk\, k^2 P(k, E)$$

- The momentum distribution (need to have good energy resolution)

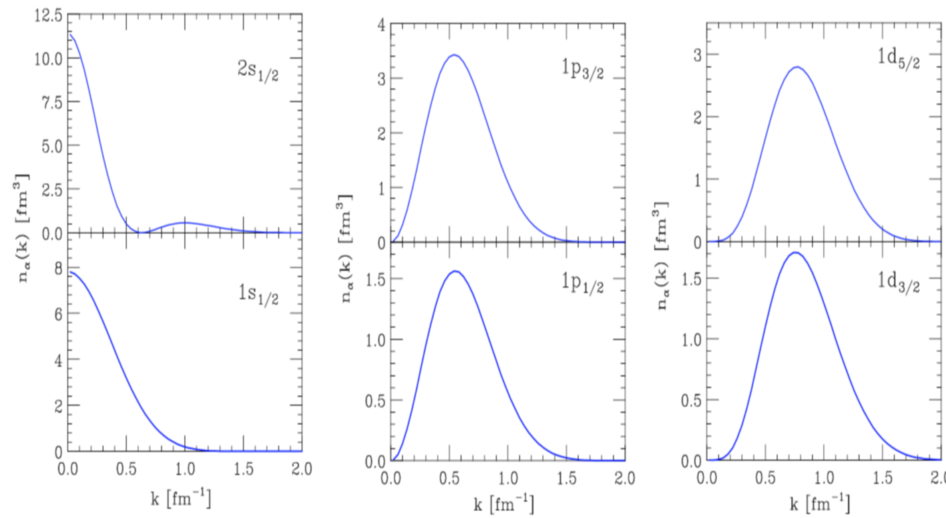

> ➢ Kinematic region for argon
> 6 MeV ≲ E_m ≲ 60 MeV
> $\mathbf{p}_m$ ≲ 350 MeV

Extracting Spectral Function from Data

- Cross section within the Plane Wave Impulse Approximation (PWIA) scheme:

$$\frac{d\sigma_A}{dE_{e'}d\Omega_{e'}dE_p d\Omega_p} \propto \sigma_{ep} P(p_m, E_m)$$

- The spectral function extracted from the data will be

$$P_{MF}(p_m, E_m) = \sum_\alpha Z_\alpha \, |\xi_\alpha(p_m)|^2 F_\alpha(E_m - E_\alpha)$$

In the absence of correlations, $Z_\alpha \to 1$, and $F_\alpha(E_m - E_\alpha) \to \delta(E_m - E_\alpha)$.

- The correlation contribution to the spectral function of a finite nucleus of mass number A can be calculated within the Local Density Approximation (LDA):

$$P_{\rm corr}(p_m, E_m) = \int d^3r \; \rho_A(\mathbf{r}) P^{NM}_{\rm corr}(p_m, E_m; \rho = \rho_A(\mathbf{r}))$$

- In Kahlen-Lehman representation: the full LDA spectral function is given by the sum

$$P(p_m, E_m) = P_{MF}(p_m, E_m) + P_{\rm corr}(p_m, E_m)$$

$$n(p_m) = \int dE \; P(p_m, E_m)$$

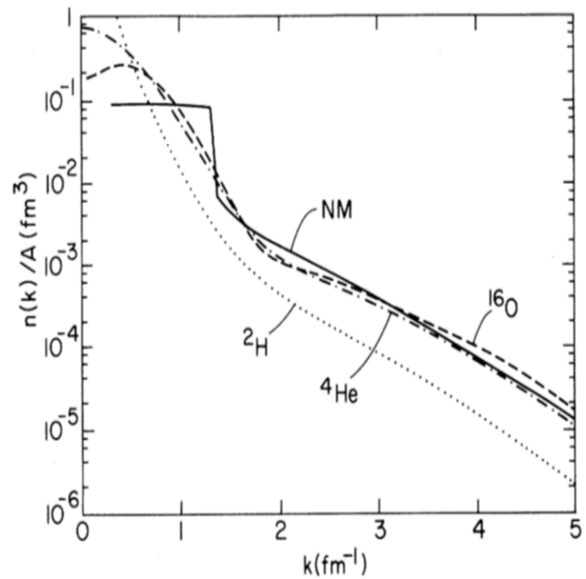

O. Benhar, S. C. Pieper, V. R. Pandharipande, Rev. Mod. Phys. 65, 817 (1993).

HALL A Schematics

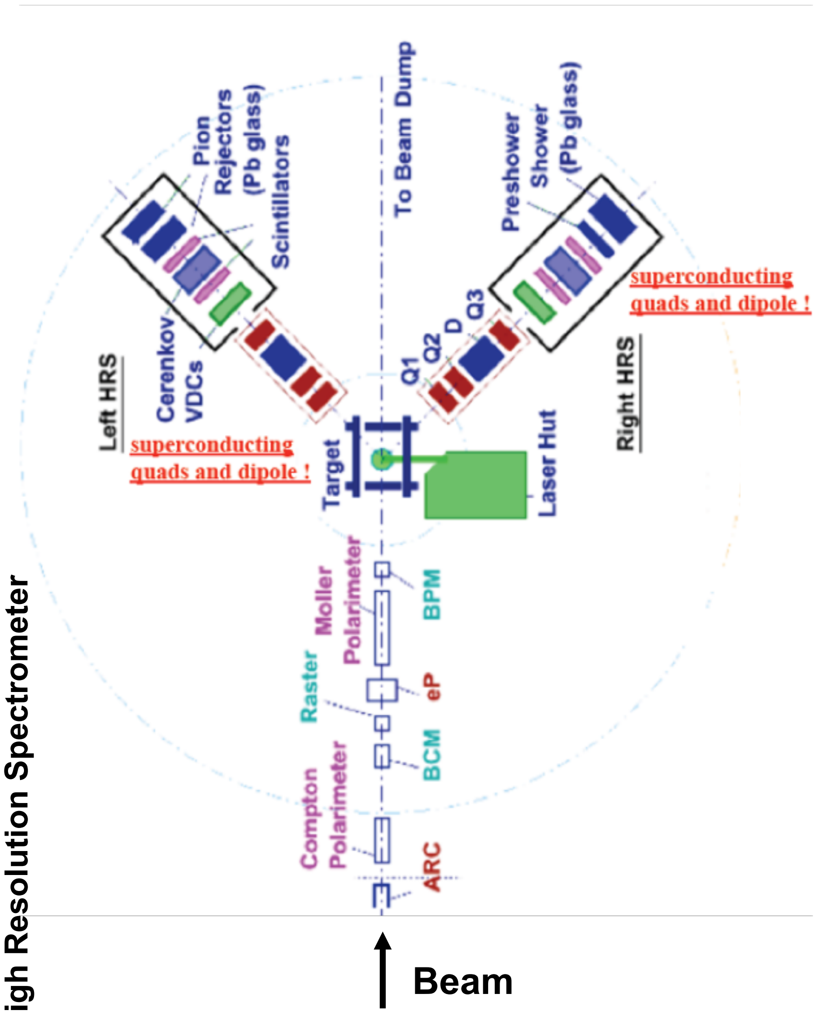

HRS: High Resolution Spectrometer

High Resolution Spectrometer

Superconducting magnets:

- large acceptance in both angle and momentum
- excellent resolution in position and angle

Detector Package:

- <u>Vertical Drift Chambers:</u>
  - high resolution tracks reconstruction (position and direction)
- <u>Scintillators:</u>
  - trigger to activate the data-acquisition electronics
  - precise timing information for time-of-flight measurements and coincidence determination
- <u>Cherenkov:</u>
  - The particle identification, obtained from a variety of Cherenkov type detectors (aerogel and gas) and lead-glass shower counters

HALL A Schematics

High Resolution Spectrometer

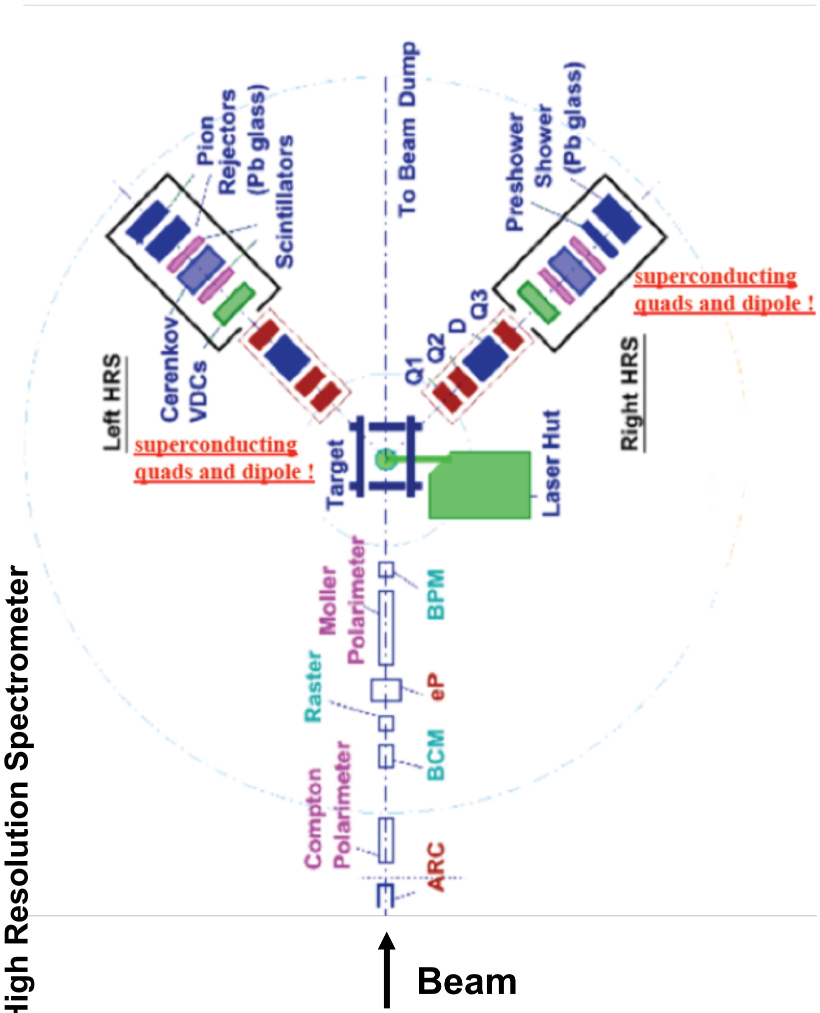

HRS: High Resolution Spectrometer

Beam Energy Resolution	5×10^{-4}
Momentum Range	0.3 – 4.0 GeV/c
Momentum Acceptance	$-4.5\% < \delta p/p < 4.5\%$
Momentum Resolution	2×10^{-4}
Angular Range	
Left Arm (electron)	12.5°-130°
Right Arm (proton)	12.5°-120°
Angular Acceptance	
Left Arm (electron)	± 30 mrad
Right Arm (proton)	±60 mrad
Angular Resolution	
Left Arm (electron)	0.5 mrad
Right Arm (proton)	1.0 mrad

Ti idea

- The reconstruction of neutrino and antineutrino energy in liquid argon detectors will require the understanding of the spectral functions describing both neutrons and protons.

- Exploiting the correspondence of the level structures, the neutron spectral function of argon can be obtained from the proton spectral function of titanium.

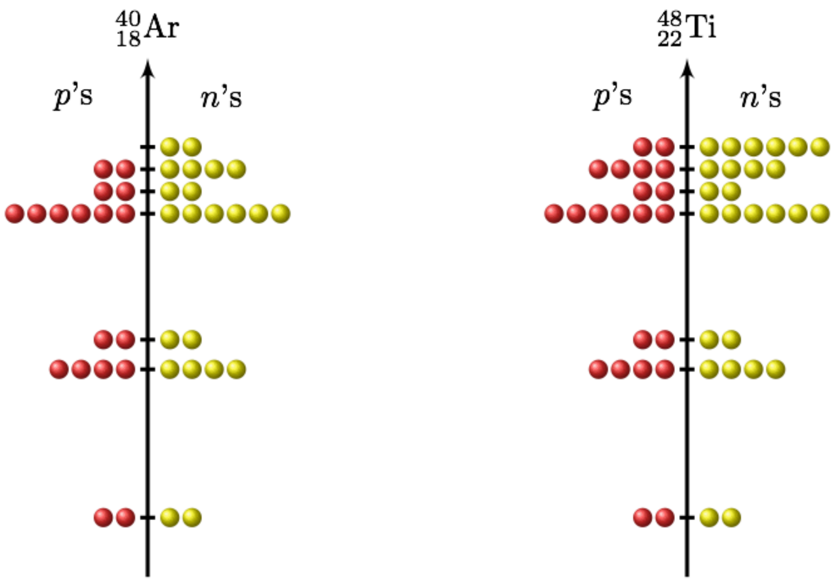

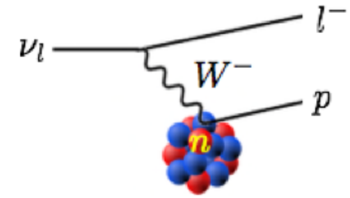

$$\nu_l + n \to l^- + p$$

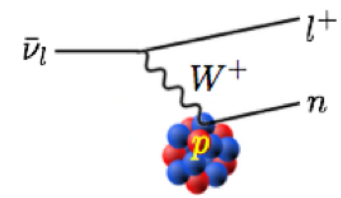

$$\bar{\nu}_l + p \to l^+ + n$$

Target Setup

Dummy target: same as the entry and exit window as the gas target

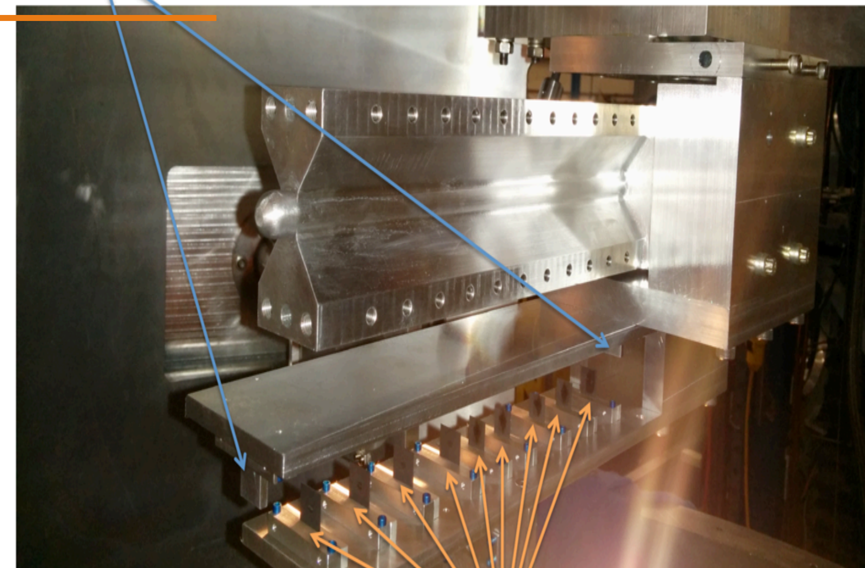

<u>Argon Target</u>

- Gas Cell
- Length = 25 cm
- Pressure = 500 PSI
- Temperature = 300 K
- Target thickness = 1.381 g cm^{-2}
- Luminosity = 4.33×10^{37} atoms cm^{-2} sec^{-1}
- Density @10μA beam current = 87%

Optical target: a series of foils of carbon (9) to check the alignment of target and spectrometers (optics)

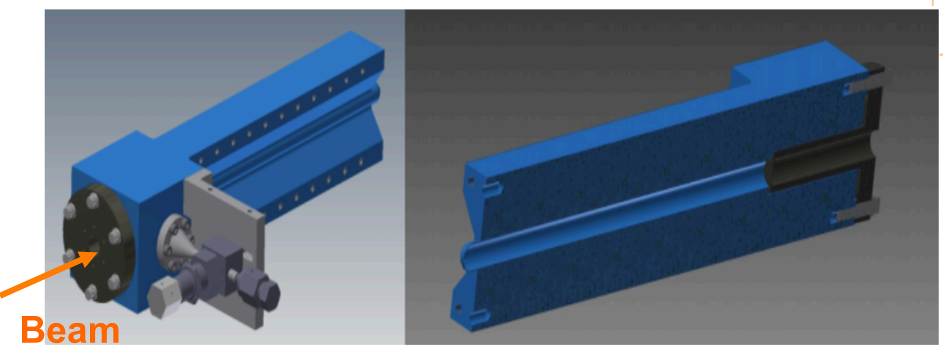

Dummy target: same as the entry and exit window as the gas target

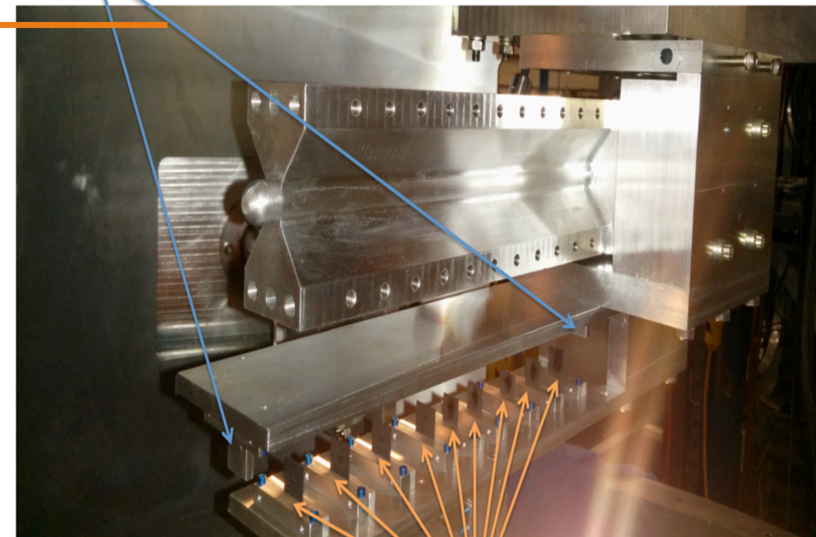

Optical target: a series of foils of carbon (9) to check the alignment of target and spectrometers (optics)

12

LEFT

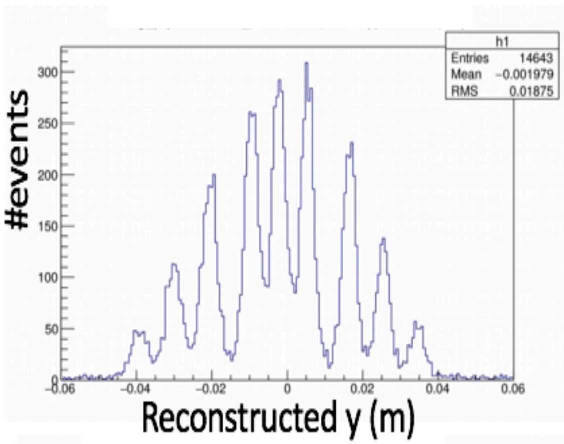

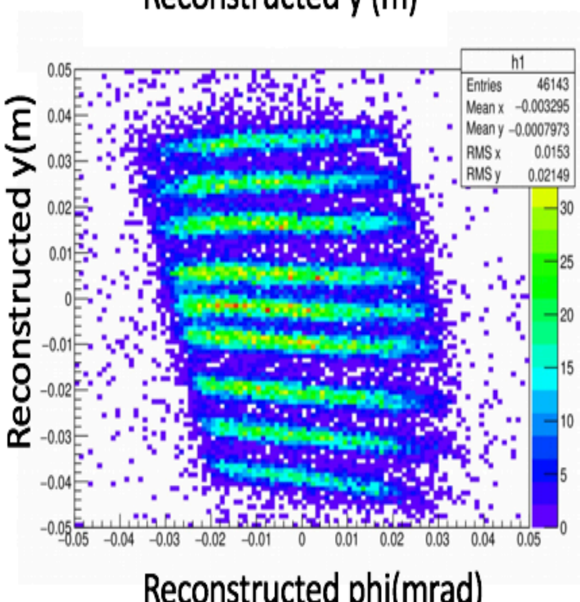

Dummy:

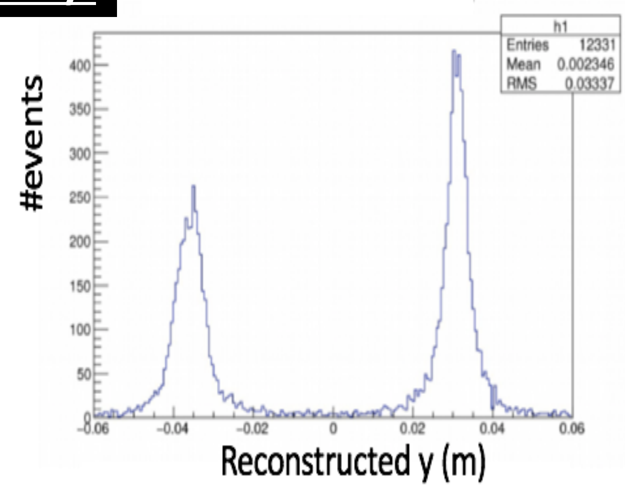

	E_e	$E_{e'}$	θ_e	P_p	θ_p	$\lvert\mathbf{q}\rvert$	p_m
	MeV	MeV	deg	MeV/c	deg	MeV/c	MeV/c
kin1	2222	1799	21.5	915	−50.0	857.5	57.7
kin3	2222	1799	17.5	915	−47.0	740.9	174.1
kin4	2222	1799	15.5	915	−44.5	658.5	229.7
kin5	2222	1716	15.5	1030	−39.0	730.3	299.7
kin2	2222	1716	20.0	1030	−44.0	846.1	183.9
kin5	2222		15.5				

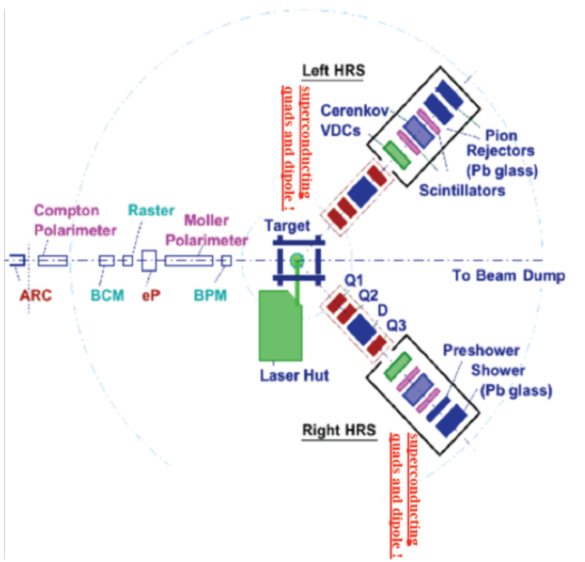

kin1

Collected Data	Hours	Events(k)
Ar	29.6	43955
Ti	12.5	12755
Dummy	0.75	955

kin3

Collected Data	Hours	Events(k)
Ar	13.5	73176
Ti	8.6	28423
Dummy	0.6	2948

kin2

Collected Data	Hours	Events(k)
Ar	32.1	62981
Ti	18.7	21486
Dummy	4.3	5075
Optics	1.15	1245
C	2.0	2318

kin4

Collected Data	Hours	Events(k)
Ar	30.9	158682
Ti	23.8	113130
Dummy	7.1	38591
Optics	0.9	4883
C	3.6	21922

kin5

Collected Data	Hours	Events(k)
Ar	12.6	45338
Ti	1.5	61
Dummy	5.9	16286
Optics	2.9	160

kin5 - Inclusive

Collected Data	Minutes	Events(k)
Ar	57	2928
Ti	50	2993
Dummy	56	3235
C	115	3957

	E_e	$E_{e'}$	θ_e	P_p	θ_p	$\|\mathbf{q}\|$	p_m
	MeV	MeV	deg	MeV/c	deg	MeV/c	MeV/c
kin1	2222	1799	21.5	915	−50.0	857.5	57.7
kin3	2222	1799	17.5	915	−47.0	740.9	174.1
kin4	2222	1799	15.5	915	−44.5	658.5	229.7
kin5	2222	1716	15.5	1030	−39.0	730.3	299.7
kin2	2222	1716	20.0	1030	−44.0	846.1	183.9
kin5	2222		15.5				

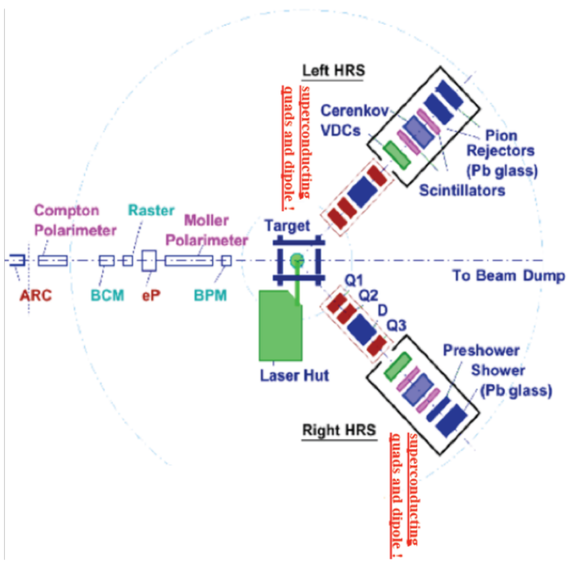

kin1

Collected Data	Hours	Events(k)
Ar	29.6	43955
Ti	12.5	12755
Dummy	0.75	955

kin3

Collected Data	Hours	Events(k)
Ar	13.5	73176
Ti	8.6	28423
Dummy	0.6	2948

kin2

Collected Data	Hours	Events(k)
Ar	32.1	62981
Ti	18.7	21486
Dummy	4.3	5075
Optics	1.15	1245
C	2.0	2318

kin4

Collected Data	Hours	Events(k)
Ar	30.9	158682
Ti	23.8	113130
Dummy	7.1	38591
Optics	0.9	4883
C	3.6	21922

kin5

Collected Data	Hours	Events(k)
Ar	12.6	45338
Ti	1.5	61
Dummy	5.9	16286
Optics	2.9	160

kin5 - Inclusive

Collected Data	Minutes	Events(k)
Ar	57	2928
Ti	50	2993
Dummy	56	3235
C	115	3957

Carbon Analysis

Analysis is mainly performed by graduate students - Hongxia Dai (VTech), Matt Murphy (VTech), and Daniel Abrams (UVA).

VDC efficiency

- Non-zero track ratio: R1
  - Cut1: Trigger, PID cut
  - $R1 = \frac{N_{track>0}}{N_{sample1}}$
- One track ratio: R2
  - Cut2: Trigger, PID cut, acceptance cut
  - $R2 = \frac{N_{track==1\&\&\,\text{y within } 5\sigma}}{N_{sample2}}$
- Efficiency=R1*R2 ~ 95 %

Calorimeter cut efficiency

- Set cut as E/p0 > 0.3
- Select Sample events
  - T3 (S0&&S2)&&(GC||PR)
  - Single track
  - Acceptance cuts
  - Cerenkov cut
- $\epsilon = \frac{\#events\ with\ E/p0>0.3}{\#sample\ events}$
- Efficiency ~ 99.9 %

Trigger Efficiency

- Production trigger: T3: (S0&&S2) && (GC||PR) [LEFT]
- Efficiency trigger: T5: (S0||S2) && (GC||PR) [LEFT]
- Selected Sample
  - T5
  - Single track cut
  - Acceptance Cuts
  - PID Cuts
- $Eff = \frac{\#events\ with\ signal\ on\ both\ S0\ and\ S2}{\#sample\ events}$ ~ 99.9 %

Cerenkov cut efficiency

- Negligible pion contamination, cer cut at 400
- Select Sample events
  - T3 (S0&&S2)&&(GC||PR)
  - Single track
  - Acceptance cuts
  - Calorimeter cut
- $\epsilon = \frac{\#events\ with\ cer>400}{\#sample\ events}$ ~ 99.9%

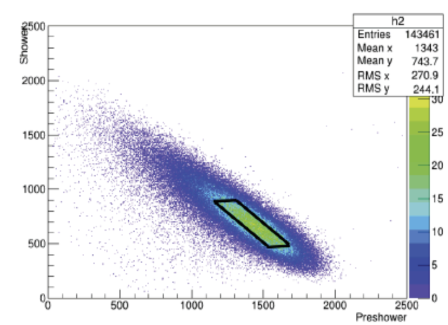

Carbon Analysis

Analysis is mainly performed by graduate students - Hongxia Dai (VTech), Matt Murphy (VTech), and Daniel Abrams (UVA).

Determining the inclusive cross section

For i[th] bin:

$$\sigma^{i}{}_{data} = \sigma^{i}{}_{model} \frac{Y^{i}{}_{data}(E',\theta)}{Y^{i}{}_{MC}(E',\theta)}$$

Where,

$$Y^{i}{}_{data} = \frac{N_s^i * prescale}{N_e * (live\ time) * \epsilon_{eff}}$$

N_s^i : Number of scattered electrons
N_e : Total number of electrons in the beam
ϵ_{eff} : Total efficiency

Carbon (e,e') inclusive cross-section

NEW RESULTS

- The carbon data allowed us to study systematics and to compare our measurements with the previous experiments.

  - Error bars up to ~ 2.5%, corresponding to the statistical (1.2%) and systematic (2.2%) uncertainties summed in quadrature.

  - **Theoretical** calculations *[Benhar et al.] are* based on the factorization ansatz dictated by the impulse approximation (IA) and the spectral function formalism. The approach does not involve any adjustable parameters, and allows for a consistent inclusion of single-nucleon interactions—both elastic and inelastic—and meson-exchange current (MEC) contributions.

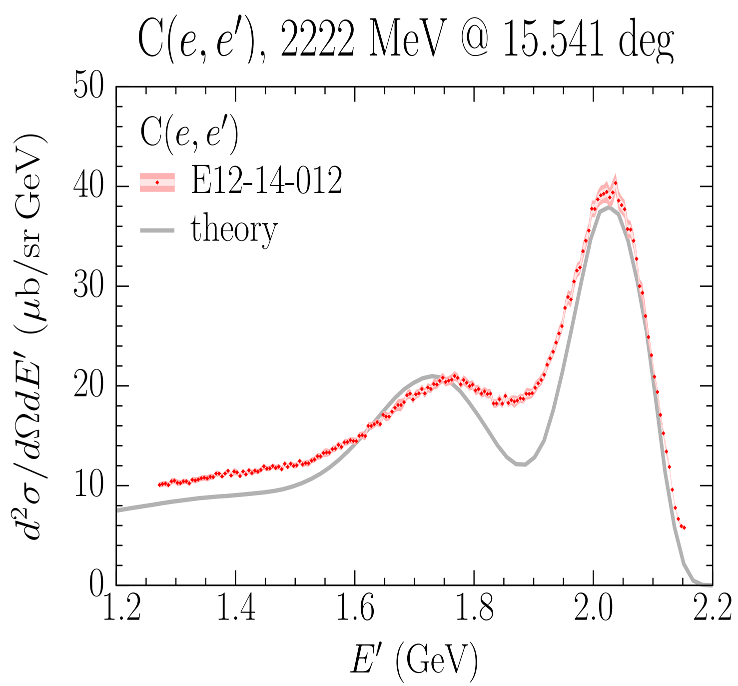

Dai, H. et al., arxiv 1803.01910.

Carbon (e,e') inclusive cross-section

NEW RESULTS

- The y-scaling function, F(y), obtained from the cross section measured by the E12-14-012 experiment to those obtained from the previous data spanning a kinematical range corresponding to $0.20 \lesssim Q^2 \lesssim 1.8$ GeV^2.

Dai, H. et al., arxiv 1803.01910.

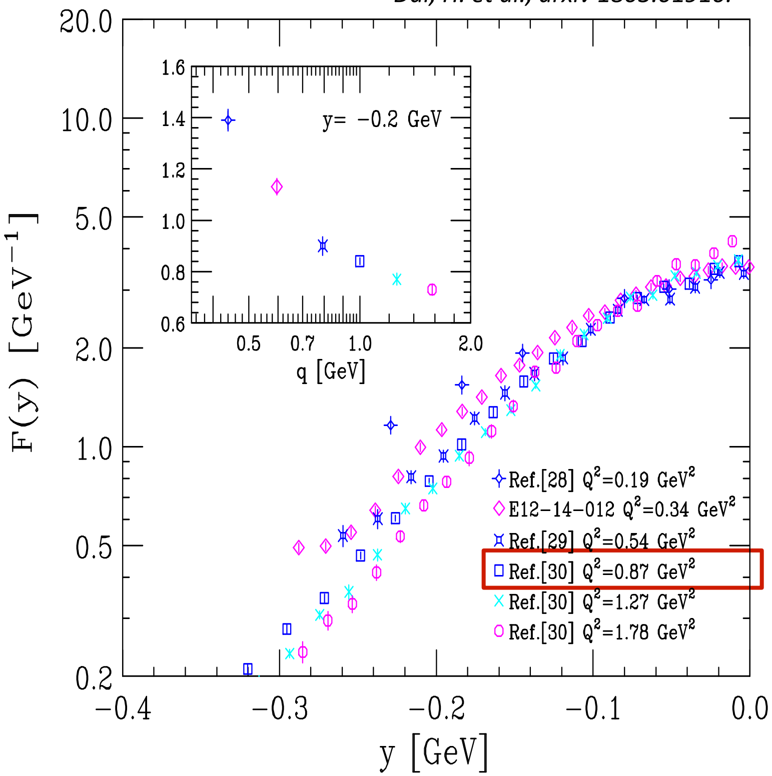

[28] J. S. O'Connell et al., Phys. Rev. C 35, 1063 (1987).
[29] R. M. Sealock et al, Phys. Rev. Lett. 62, 1350 (1989).
[30] D. B. Day et al, Phys. Rev. C 48, 1849 (1993).

- At *y* ≈ 0, the data exhibit a remarkable scaling behavior corresponding to $\omega \approx Q^2/2M$.
- At large negative values of *y*, a sizable scaling violations, to be mainly ascribed to FSI, are observed.
- The F(y) as a function of q, at y = −0.2 GeV, demonstrates that in the kinematical setup of our experiment, corresponding to |q| ≈ 600 MeV, the effects of FSI are still significant.
- Our results are fully consistent with those of previous experiments.

Titanium (e,e') inclusive cross-section

NEW RESULTS

- The first electron-scattering data ever collected on titanium target.

- Error bars up to ~ 2.75%, corresponding to the statistical (1.65%) and systematic (2.2%) uncertainties summed in quadrature.

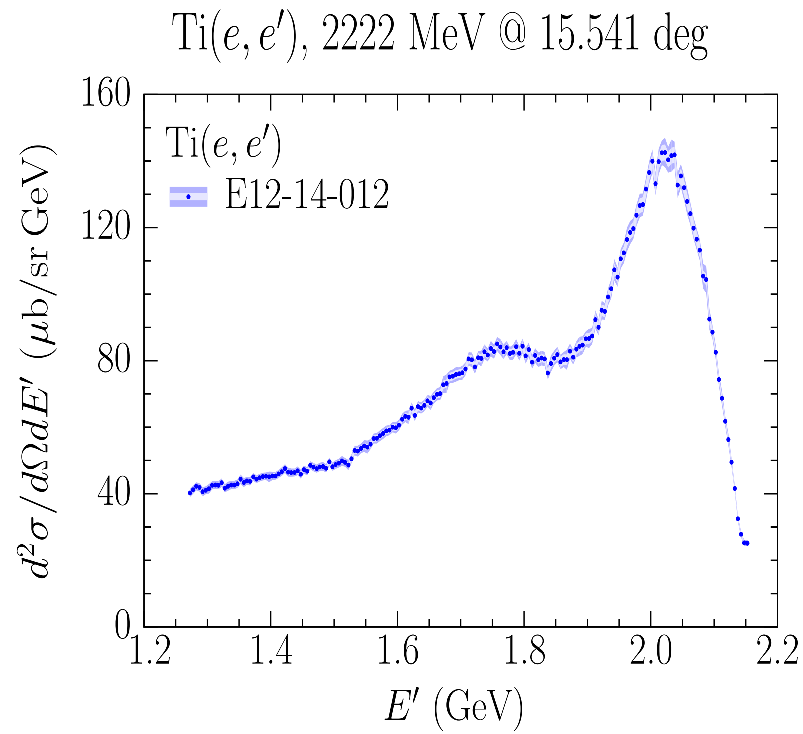

Dai, H. et al., arxiv 1803.01910.

Comparing Ti (e,e') and C(e,e') cross-section

$$\frac{d^2\sigma}{d\Omega dE'}/[Z\sigma_{ep} + (A-Z)\sigma_{en}]$$

- The quantities σ_{ep} and σ_{en} are the elementary electron-proton and electron-neutron cross sections in the QE channel stripped of the energy-conserving delta function.

- The difference between the results obtained using the measured carbon and titanium cross sections reflect different nuclear effects.

Dai, H. et al., arxiv 1803.01910.

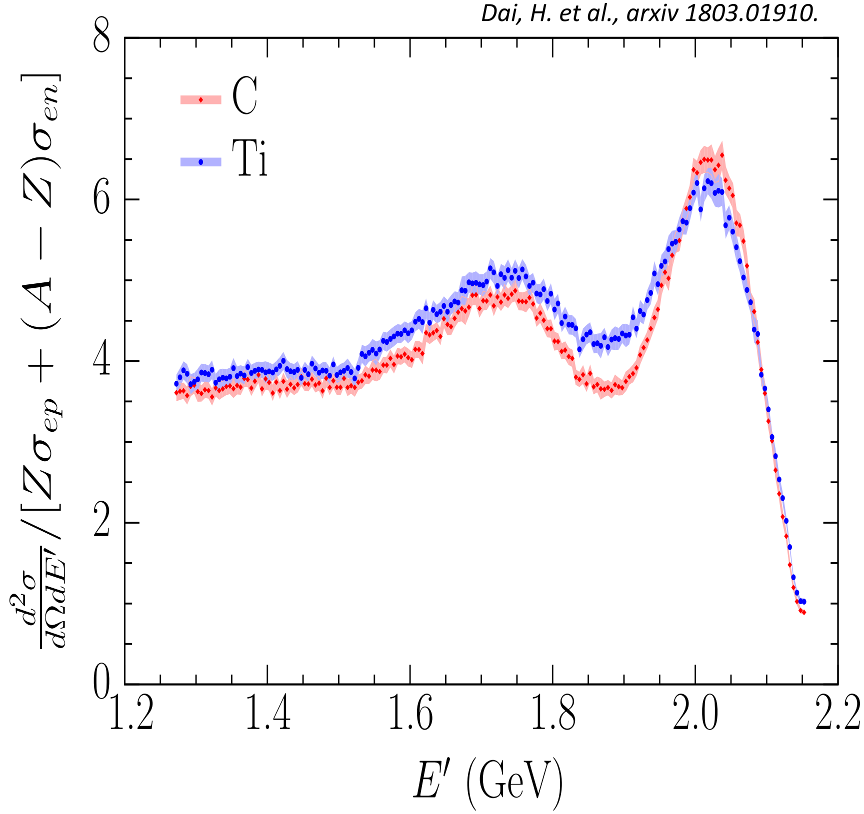

Comparing Ar (e,e'), Ti (e,e') and C(e,e') cross-section

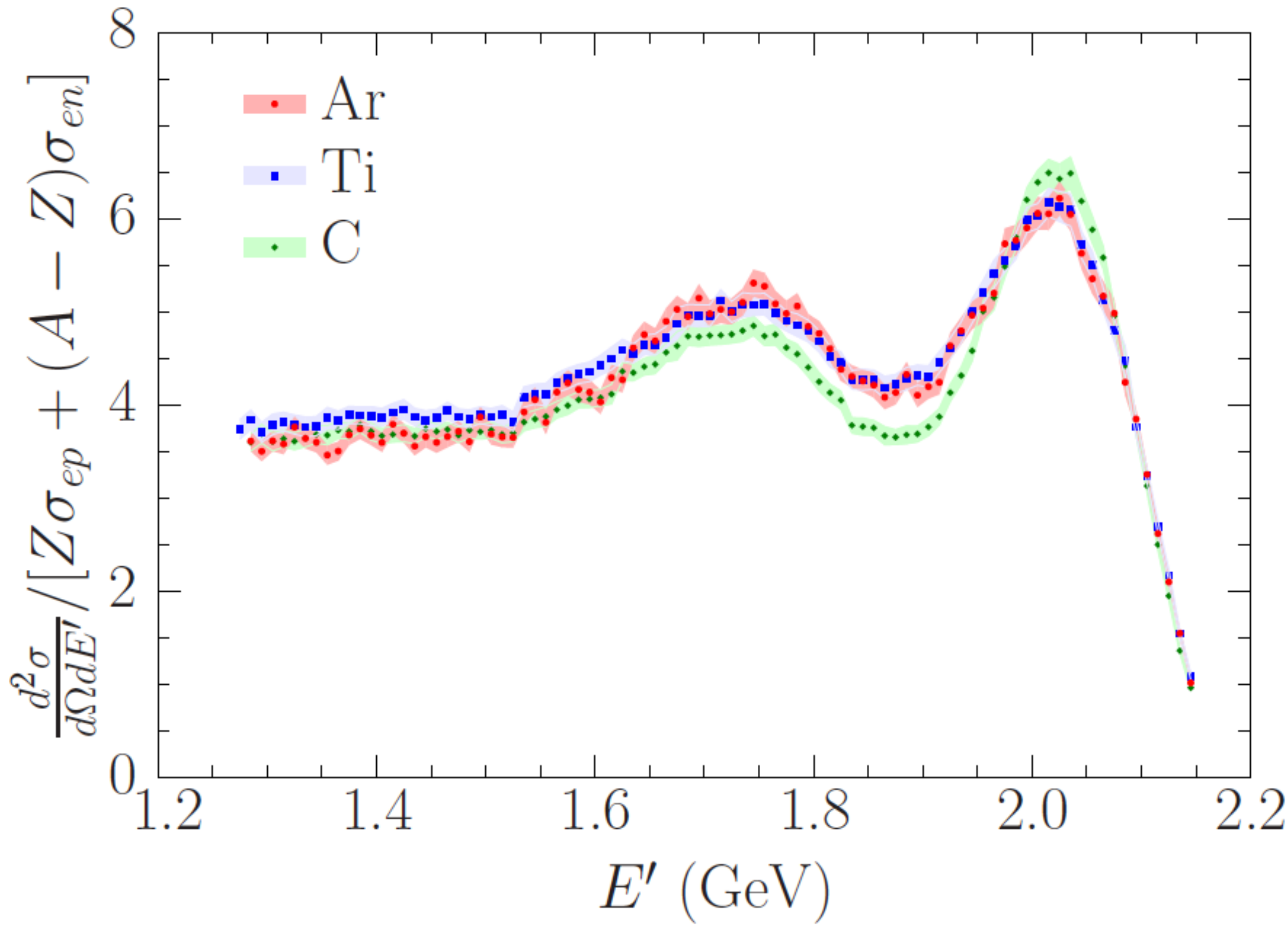

Conclusions

- Neutrino cross section and nuclear models influence how we reconstruct the neutrino energy and how we cna identify experimentally neutrinos
- Energy reconstruction essential for precision determination of neutrino oscillation parameters and neutrino-hadron cross sections
- The Impact on neutrino oscillation experiments due to nuclear models, what they are and how they are implemented is not negligible (order 10%)
  - neutrino event generators use almost same data set so there are correlations that are non-negligible
  - using wrong models affect neutrino oscillation parameters determination